# Residual cerebral activity and behavioural fragments can remain in the persistently vegetative brain

Nicholas D. Schiff,[1] Urs Ribary,[4] Diana Rodriguez Moreno,[5] Bradley Beattie,[5] Eugene Kronberg,[4] Ronald Blasberg,[5] Joseph Giacino,[6] Caroline McCagg,[6] Joseph J. Fins,[2,3] Rodolfo Llinás[4] and Fred Plum[1]

*Departments of [1]Neurology and Neuroscience, [2]Medicine and [3]Psychiatry, Weill Medical College of Cornell University, [4]Center for Neuromagnetism, Department of Physiology and Neuroscience, New York University School of Medicine, [5]Memorial Sloan Kettering Cancer Center, Department of Neurology, New York, [6]JFK Medical Center, JFK Johnson Rehabilitation Institute, Center for Head Injuries, Edison, New Jersey, USA*

*Correspondence to: Nicholas D. Schiff, MD, Assistant Professor, Department of Neurology and Neuroscience, Weill College of Medicine of Cornell University, 1300 York Avenue, New York, NY 10021, USA E-mail: nds2001@med.cornell.edu*

## Summary

This report identifies evidence of partially functional cerebral regions in catastrophically injured brains. To study five patients in a persistent vegetative state (PVS) with different behavioural features, we employed [18F]fluorodeoxyglucose-positron emission tomography (FDG-PET), MRI and magnetoencephalographic (MEG) responses to sensory stimulation. Each patient's brain expressed a unique metabolic pattern. In three of the five patients, co-registered PET/MRI correlate islands of relatively preserved brain metabolism with isolated fragments of behaviour. Two patients had suffered anoxic injuries and demonstrated marked decreases in overall cerebral metabolism to 30–40% of normal. Two other patients with non-anoxic, multifocal brain injuries demonstrated several isolated brain regions with relatively higher metabolic rates, that ranged up to 50–80% of normal. Nevertheless, their global metabolic rates remained <50% of normal. MEG recordings from three PVS patients provide clear evidence for the absence, abnormality or reduction of evoked responses. Despite major abnormalities, however, these data also provide evidence for localized residual activity at the cortical level. Each patient partially preserved restricted sensory representations, as evidenced by slow evoked magnetic fields and gamma band activity. In two patients, these activations correlate with isolated behavioural patterns and metabolic activity. Remaining active regions identified in the three PVS patients with behavioural fragments appear to consist of segregated corticothalamic networks that retain connectivity and partial functional integrity. A single patient who suffered severe injury to the tegmental mesencephalon and paramedian thalamus showed widely preserved cortical metabolism, and a global average metabolic rate of 65% of normal. The relatively high preservation of cortical metabolism in this patient defines the first functional correlate of clinical–pathological reports associating permanent unconsciousness with structural damage to these regions. The specific patterns of preserved metabolic activity identified in these patients do not appear to represent random survivals of a few neuronal islands; rather they reflect novel evidence of the modular nature of individual functional networks that underlie conscious brain function. The variations in cerebral metabolism in chronic PVS patients indicate that some cerebral regions can retain partial function in catastrophically injured brains.

**Keywords**: PET; MRI; consciousness; magnetoencephalography; persistent vegetative state

**Abbreviations**: AEF = auditory evoked magnetic field; CSPTC = corticostriatopallidal–thalamocortical; FDG-PET = [18F]fluorodeoxyglucose-positron emission tomography; MEF = magnetic evoked field; MEG = magnetoencephalography; PVS = persistent vegetative state; rCMRglu = regional cerebral metabolic rate for glucose; ROI = region (volume) of interest; SEF = somatosensory evoked magnetic field

# Introduction

Severe brain injuries constitute an epidemic public health problem affecting >100 000 Americans annually ( Winslade, 1998; NIH Consensus Panel, 1999). For some of these patients, it is becoming more probable that novel therapeutic avenues may develop to address their neurological disabilities. At present, however, patients who suffer complex brain injuries resulting from traumatic, anoxic/hypoxic or axonal-shearing disruptions of cerebral function are viewed as a homogeneous group with hopeless outcomes. This outlook has resulted in few attempts at neurobiological treatments to raise their functional capacities. Moreover, few investigations have been directed to this question. As an unfortunate result, understanding of preserved cerebral functions in severely damaged brain remains at the borderline of professional expertise in the clinical neurosciences (Beresford, 1997).

This study identifies unexpected residual cerebral activity in patients in a chronic persistent vegetative state (PVS). The approach taken departs from classical neurological efforts to identify focal brain injuries associated with losses of behaviour. Our present results highlight a novel corollary of the modular nature of brain organization: the presence of a given module, even in isolation, should support some aspects of the specific functions lost in its absence. We show partial preservations of brain function that correlate with isolated behaviours in chronically unconscious brains and illustrate that an 'inverse' or reciprocal method of clinical–pathological correlation is equally successful.

PVS describes a sustained human behavioural condition in which awareness of self or environment is absent, despite preservation of autonomic bodily and brainstem functions and recurrently expressed sleep/wake cycles (Jennett and Plum, 1972). Their lack of interactive behaviours notwithstanding, many patients in a PVS grimace, tear, vocalize or generate fragmentary movement patterns often hard to categorize as non-purposeful without careful and repeated examination. In most cases, these fragmentary behavioural patterns can be related to limbic and brainstem networks that lie outside of the corticothalamic systems that have been overwhelmingly injured in PVS patients (Multi-Society Task Force on PVS, 1994; Adams *et al.*, 2000). Occasionally, patients in a PVS may express isolated behavioural fragments clearly generated at a forebrain level. Our index case consisted of such a unique vegetative patient who randomly produced occasional single words (Schiff *et al.*, 1999). In this patient, isolated regions of preserved cerebral metabolic activity and thalamocortical transmission were associated with remnants of the human language system. These findings led us to evaluate additional PVS patients with multimodal imaging techniques in order to determine in detail what cerebral activity may remain in patients with catastrophic brain injuries.

Past studies of resting cerebral brain metabolism utilizing [$^{18}$F]fluorodeoxyglucose-positron emission tomography (FDG-PET) in PVS have consistently demonstrated diffuse, uniformly reduced cerebral metabolic activity (Levy *et al.*, 1987; DeVolder *et al.*, 1990; Tommasino *et al.*, 1995; Rudolf *et al.*, 1999; Laureys *et al.*, 1999). We describe here the first evidence of reciprocal clinical–pathological correlation with regional differences of quantitative cerebral metabolism. We also employ magnetoencephalography (MEG) to analyse dynamic aspects of source activations in the PVS patients. MEG represents a unique functional imaging technique that allows identification of spatiotemporal sources of brain activations associated with specific frequency bands during sensory processing (Regan, 1989; Ribary *et al.*, 1991, 1999; Baumgartner *et al.*, 1995; Llinás *et al.*, 1999). This diagnostic protocol was designed to examine the possible persistence of remaining coherent neuronal network activity as either localized slow evoked fields or coherent high-frequency (gamma band) activity. The MEG data from the PVS patients indicate partially preserved but delayed and abnormally incomplete coherent dynamic brain activity. The combination of techniques employed here allows us to assess the residual network properties that underlie the expression of fractional behaviour observed in three of the chronic vegetative patients presented here.

The presence of preserved forebrain activity in chronic unconsciousness provides a possible window onto the functions of isolated modules in the human brain. We further discuss the results of these imaging studies in the context of the diagnostic evaluation of complex brain injuries and the underlying mechanisms of vegetative and other states of severe brain injury.

# Methods
## *Protocol*

We chose five patients from over 60 possible vegetative patients using several inclusion criteria. We selected patients between the ages of 18 and 70 years, who were systemically healthy, capable of independent ventilation, in a PVS for at least 6 months and for whom a legally authorized surrogate could be identified to provide informed consent for a complete neurological and general physical examination and brain imaging studies. As noted below, in addition to meeting these criteria, Patients 1–3 exhibited unusual behavioural features. No other PVS patients evaluated showed similar behavioural fragments, and Patients 1–3 were selected in part because of these additional findings in the history and examination. Only the five PVS patients reported here were studied under the protocol.

We conducted comprehensive evaluations during five hospitalization days in the Cornell-New York Presbyterian Hospital Clinical Research Center. Patients were studied with MRI, PET and MEG. Other clinical evaluations included 24-h video-EEG monitoring and application of selective evoked potential analyses. PET studies were obtained to support the

clinical diagnosis of the vegetative state. Investigative imaging with MRI and MEG was performed after obtaining approval for the protocol from the Institutional Review Board (IRB) of New York Presbyterian Hospital, the Bellevue Hospital IRB and The New York University Hospital IRB and consent from the patient's legally authorized surrogate. All functional brain imaging studies were done under physician guidance.

### FDG-PET imaging and analysis

All scans were performed on a General Electric ADVANCE PET scanner (Milwaukee, Wisc.) using its 2D (septa-in) mode with a span of 7. The camera has a field of view of 55 cm transaxially and 15.2 cm axially. We reconstructed images using the filtered back projection algorithm and the default filter settings to achieve a transaxial resolution of 3.8 mm FWHM (full width half maximum) on the camera's central axis, which increased to 7.3 mm at a radial distance of 20 cm. The average axial resolution ranges from 4.0 mm FWHM at the centre of the field of view to 6.6 mm at 20 cm (DeGrado *et al.*, 1994).

We studied all patients at rest, in a supine position, with their eyes open. Tube feedings were withheld for 6 h prior to the study and each patient received an infusion of physiological saline during the study. Each patient received a bolus intravenous injection of ~270 MBq [$^{18}$F]FDG. Following the injection, we took a series of 25 blood samples (over a period of 60 min) from an arterial line placed temporarily in the patient's left radial artery. The samples were immediately placed on ice and shortly thereafter centrifuged and assayed for plasma [$^{18}$F]FDG concentration. We took additional blood samples at 20-min intervals and assayed them for plasma glucose concentration.

Starting 40 min after the injection, a 20-min PET emission acquisition of the brain was performed, followed by a 10-min transmission scan. We reconstructed these data into images using the standard GE software with corrections for scatter, dead-time, decay, randoms, detector inhomogeneity and attenuation (measured), including a correction for the emission data that were present during the transmission scan. We determined regional cerebral metabolic rate for glucose (rCMRglu) using the FDG autoradiographic method (Phelps *et al.*, 1979; Sokoloff *et al.*, 1977). For Patient 1 only, after the first 40 min following injection (and concurrent blood sampling), a single low dose of lorazepam (2 mg via percutaneous gastrostomy tube) was given to quiet spontaneous movements. The medication was given only after the plateau in the uptake of FDG had been reached.

### Image registration

We achieved co-registrations by a rigid-body transformation that registered each patient's PET brain images to their MRIs using the Mutual Information Criteria method (Collignon *et al.*, 1995). Following the transformation to the MRI coordinate system, the PET rCMRglu images were resliced, using trilinear interpolation, along the planes of the MRIs.

### Region of interest analysis

Raw images for each patient showed clear regional variations and asymmetries. To delineate these visible differences in the raw, we developed a simple regional analysis. For each patient, volumes of interest (ROIs) were drawn on selected structures identified on the patient's MRIs. We applied these ROIs to the co-registered (i.e. resliced) rCMRglu images and determined for each ROI the mean, the standard deviation and the maximum of the PET voxels within the ROI. These values were compared with values from a database of normal rCMRglu values obtained from 18 normal subjects scanned with the same generation GE ADVANCE PET camera and analysed using similar procedures in studies conducted at The North Shore University Hospital by Dhawan *et al.* (1998). Two structures, orbitofrontal gyrus and superior parietal lobe, were not represented in the database of normals. Normal values for these structures were determined using data from five normal subjects, a randomly selected subset of the original 18. The percentages of normal values were calculated on a voxel-by-voxel basis using the corresponding normal values for each brain region. Thresholded images of percentage of normal rCMRglu were displayed using a simple colour scale, overlaid onto the corresponding registered MRIs. For the non-anoxic patients, voxel values above a threshold of 55% were displayed using four colours, three colours corresponding to 10% of normal CMRglu ranges from 55 to 85%, and a fourth colour corresponding to the 85–100% range. Images utilizing this colouring scheme were superimposed directly on the registered MRIs. The anoxic patient data were displayed similarly, except that a threshold of 35% and two additional colours for the ranges of 35–45 and 45–55% were used.

### MEG recordings and analysis

We used a double dewar 74-channel MEG system (4D Neuroimaging Inc., San Diego, Calif.) in one patient (Patient 3), and a whole-head 148-channel MEG system (4D Neuroimaging Inc., San Diego, Calif.) in the remaining three patients studied using MEG and all control subjects. Evoked magnetic activity, in response to bilateral auditory or unilateral somatosensory stimulation, was evaluated for both hemispheres (Mogilner *et al.*, 1993; Joliot *et al.*, 1994). The patients and controls were gently placed supine on the instrument's bed and the magnetic sensor array positioned over the head. Binaural auditory stimuli comprised of random clicks (10 kHz, squarewave) were delivered to the subject through plastic tubing. Tactile stimulation was delivered via conventional airpuff stimulators (Rezai *et al.*, 1996) attached to the subject/patient's left or right thumb. Auditory and somatosensory stimuli were presented with interstimulus intervals of 300 ± 30 or 500 ± 50 ms, respectively. MEG

activity was recorded from 70 ms before to 180 ms after the onset of the auditory stimulus (1000 epochs), and from 150 ms before to 250 ms after the onset of each tactile stimulus (250 epochs), with a bandpass of 1–400 Hz and a sampling rate of 1017 Hz. In Patient 3, MEG activity was recorded with a 74-channel system from 50 ms before to 200 ms after the onset of the tactile stimulus delivered to the left index finger (250 epochs). Transient responses were averaged using the onset of the stimulus as a trigger (Joliot *et al*., 1994). Single-dipole analysis procedures ( Sarvas, 1997) were used to estimate sources of primary sensory areas, which were co-registered and overlaid on MRI slices, based on a transformation and rotation of the head-based coordinate system with respect to natural landmarks and the attachment of vitamin E pills during MRI scanning (Rezai *et al*., 1996). Co-registered PET–MRI data (above) were compared with MEG–MRI co-registered dipoles.

Evoked and averaged MEG data were filtered in the 3–40 Hz range to optimize the display of classical magnetic evoked field (MEF) components within the time window analysed. The data additionally were wide-band filtered at 20–50 Hz specifically to extract the gamma band response from the lower frequency activity, which correlated with the high-frequency rhythm near 40 Hz in the raw data. Main deflections in averaged and filtered data were analysed and, by using the single dipole model (Williamson and Kaufman, 1990; Sarvas, 1997), temporal source activations were computed and overlaid onto MRIs. The single dipole represents mostly the activity at the cortical level, which is part of a thalamocortical network activity in the sensory regions. However, the appearance of a cortical response already provides evidence for a locally synchronized and coherent response having some intact thalamocortical connections, otherwise the cortical activity would be desynchronized and too small to be detected by MEG.

## MEG recordings from control subjects

Auditory evoked magnetic fields (AEFs) in control subjects demonstrated a classical N100 deflection at ~100 ms best seen in the 3–40 Hz range (Fig. 1A), which is well known to localize to the Heschl's gyrus within both hemispheres (Reite *et al*., 1982; Romani *et al*., 1982; Yamamoto *et al*., 1988; Williamson and Kaufman, 1990). Unfiltered data further indicated that in addition to a large low-frequency response, a distinct temporal pattern in the gamma band was present and could be extracted, as seen in filtered data (20–50 Hz). The gamma band activation indicated the clear time-locked response that occurs with respect to a given auditory stimulus, followed by a stable synchronized and coherent time-locked response. We had earlier described the gamma band response produced by a single stimulus as a 2.5 oscillatory cycle, demonstrating ~2.5 oscillations at 40 Hz (Joliot *et al*., 1994). Earlier reports localized the main components of the temporal sequence of the gamma band response to primary auditory
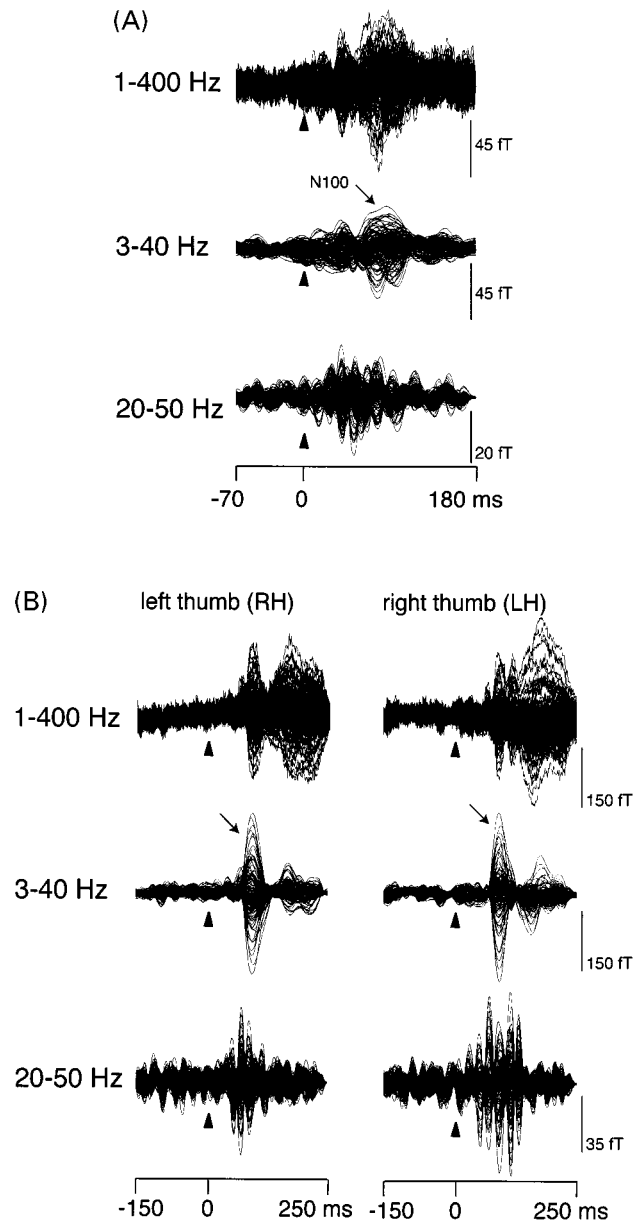


**Fig. 1** (**A**) Healthy control subject auditory stimulation: auditory evoked magnetic fields (AEFs) following bilateral auditory stimulation. Averaged waveforms are superimposed for all MEG channels and displayed unfiltered (1–400 Hz), and filtered at 3–40 and 20–50 Hz. In addition to classical AEF components, best seen in the 3–40 Hz range (N100), these data indicate a distinct temporal pattern in the gamma band as seen in filtered data (20–50 Hz). The gamma band activation represents a well-known time-locked activity with respect to one auditory stimulus. (**B**) Healthy control subject somatosensory stimulation: contralateral somatosensory evoked magnetic fields (SEFs) following tactile stimulation of the left (left column) or right thumb (right column). Averaged waveforms are superimposed for all MEG channels and displayed unfiltered (1–400 Hz), and filtered at 3–40 and 20–50 Hz. In addition to classical SEF components (main peak indicated by an arrow), best seen in the 3–40 Hz range, these data indicate a distinct temporal pattern in the gamma band as seen in filtered data (20–50 Hz). The gamma band activation represents a known time-locked activity with respect to one somatosensory stimulus.

areas (Makela *et al.*, 1987; Weinberg *et al.*, 1988; Ribary *et al.*, 1989, 1991; Pantev, 1991).

The classical somatosensory evoked magnetic fields (SEFs), best seen in the 3–40 Hz range (Fig. 1B), indicate a main peak at ~90 ms (Rezai *et al.*, 1996) well known to be localized to the contralateral area 3b within primary somatosensory area S1 following left or right tactile stimulation (Hari *et al.*, 1984; Okada *et al.*, 1984; Sutherling *et al.*, 1988; Wood *et al.*, 1988; Suk *et al.*, 1991; Mogilner *et al.*, 1993; Nakamura *et al.*, 1998). The findings further indicated a distinct temporal sequence of source activations in the higher frequency (20–50 Hz) range, representing a time-locked gamma band activity in response to somatosensory stimuli, followed by a synchronized and coherent response. The main component of the temporal sequence of the gamma band response has also been localized within the primary somatosensory area (Weinberg *et al.*, 1988; Desmedt *et al.*, 1994; Pfurtscheller *et al.*, 1994; Sauvé *et al.*, 1998).

# Results of brain imaging and functional interpretations
## Patient 1

Six months after his post-operative anoxic injury, Patient 1 was mute, unresponsive to visual, auditory or cutaneous stimuli, but during wakefulness expressed continuous, mild to moderate choreiform movements of the head, trunk and extremities (Table 1). MRI revealed large ventricles and thin bands of cortical tissue indicating laminar necrosis that particularly involved the posterior parietal and occipital regions. The caudate nuclei appeared bilaterally atrophic.

During FDG-PET imaging studies, the patient was awake and expressed choreiform activity. Figure 2A illustrates the PET data obtained from Patient 1. Anterior forebrain structures revealed relatively higher metabolic activity than posterior regions. Figure 2B shows a histogram of mean values of regional cerebral metabolic rate (rCMRglc) per anatomic area for Patient 1 as a percentage of normal values. Metabolic rates range from 21 to 50% of normal rCMRglc, with average CMR for the whole brain of 31% of normal. Increased resting metabolic rates above the average CMR are observed in the pons, cerebellum, medial temporal gyri, mesencephalon (note significant tegmental activation), putamen, right orbitofrontal gyrus, right caudate nucleus and thalami. Figure 2C illustrates the voxels expressing >35% of normal rCMRglc co-registered onto the patient's MRIs. Voxels with peak metabolic rates that exceeded 50% of normal were identified in the pons, midbrain (Fig. 2Ca), cerebellum (Fig. 2Cb), medial temporal cortex, thalami (Fig. 2Cc) and right orbitofrontal cortex (Fig. 2Cf). Average metabolic rates for these structures with higher peak values ranged from 32% of normal (left thalamus) to 50% of normal (pons). The predominance of anterior structures seen in Fig. 2A is shown in Fig. 2C by the

relatively increased metabolic activity observed in bilateral orbitofrontal and medial frontal cortex (note that while peak values here at >35% of normal are above the 31% global average, averages for these structures in Fig. 2B are not).

## Interpretation

The increased metabolic rates observed in several anterior brain structures compared with posterior brain regions on Patient 1 (Fig. 2C) and his associated behaviour suggest that Patient 1 represents a vegetative variation of hyperkinetic mutism, a recently described neurological syndrome (Inbody and Jankovic, 1986; Schiff and Plum, 2000). Hyperkinetic mutism follows bilateral destruction of temporal–parietal–occipital junctions and is characterized by totally unrestrained but coordinated motor activity in the absence of self-awareness, and limited interaction with the environment (Inbody and Jankovic, 1986; Mori and Yamadori, 1989; Fisher, 1983). Unlike hyperkinetic mutism, the unconscious motor activity in this patient runs free, without any evidence of regulation or purposeful aim. The greater degree of posterior cortical injuries in Patient 1, as evidenced by both differences in rCMRglc and patterns of laminar necrosis on MRI, supports this comparison. Moreover, this interpretation is supported further by the known clinical–pathological correlations of lesions producing different forms of akinetic mutism, an opposite condition in which patients often preserve the appearance of vigilance in a motionless state (Cairns *et al.*, 1941; see review in Schiff and Plum, 2000). As illustrated in Fig. 2D, the specific brain regions that when damaged produce varieties of akinetic mutism associate to the areas of preserved cerebral activity observed in Patient 1 [arrows schematically indicate ascending connections from brainstem to thalamus and corticostriatopallidal–thalamocortical (CSPTC) loop connections]. Forms of less classic akinetic mutism may result from bilateral injury to tegmental mesencephalic (Fig. 2Da) or paramedian thalamic (Fig. 2Dc) regions (Segarra *et al.*, 1970; Castaigne *et al.*, 1981), bilateral basal ganglia lesions (Fig. 2Dd) (Bhatia and Marsdenm 1994) and, more classically, bilateral medial and orbitofrontal cortices (Fig. 2De and f) (Nemeth *et al.*, 1988). These structures are all involved directly or indirectly in CSPTC loop circuits that also include projections from the globus pallidus interna to the intralaminar thalamic nuclei (and ventral tier) and to the pedunculo-pontine tegmental nucleus (Parent and Hazrati, 1995). All these structures show relatively high metabolic activity in Patient 1 (see Fig. 2C), consistent with this interpretation. The activation in the orbitofrontal and medial frontal cortices may represent the cortical components of these circuits. The relatively preserved metabolic activity in the medial temporal lobes is of interest but of unclear significance. Patient 1's data suggest that free-running CSPTC loops may underlie the unconscious movement disorder demonstrated in both conditions.

**Table 1** *Patient information*

| Patient (sex/age) | Duration of PVS | Clinical history | Clinical examination | Observable behaviour |
|---|---|---|---|---|
| **Anoxic injury** | | | | |
| 1 (M/52) | 6 months | Cosmetic surgery followed by post-operative asphyxia, hypotension, transient seizures, and severe hypoxaemia. Two weeks of interactive arousal followed by 6 weeks of coma with progression to PVS. | Roving eye movements. Head and eye turning to right dominate the movements. Bilateral abnormal oculovestibular reflexes (without fast component). Sluggish pupillary responses to light. Pupil dilatation in response to noxious stimuli. Noxious stimulation of the extremities and torso evokes synchronized flexion of the arms and legs with dystonic posturing. Right hemiparesis. | Continuous, spontaneous, mild to moderate non-directed choreiform movements of head, trunk and extremities during wakefulness. Mute, movements unmodulated by visual, auditory or cutaneous stimuli. |
| 2 (M/42) | 7 years | Motor vehicle accident resulting in head trauma followed by post-operative cardiopulmonary arrest. | Limbs severely spastic and contractured, with flexion at the shoulder, elbow and wrist joints as well as rigid equinovarus positioning of the legs. Failure to condition to semi-noxious stimuli (e.g. acoustic startle, repetitive glabellar taps). | Teeth clenching, groans, pupillary dilatation, facial flushing, hypertension and tachycardia in response to touch or loud noises. Soothing with soft music or voice. No response to smells or tastes, eye threats, language or noxious auditory or tactile stimuli. |
| **Traumatic injury** | | | | |
| 3 (F/49) | 25 years | Three successive haemorrhages from arterial–venous malformation in right basal ganglia and diencephalon. | Constant eye roving, pupils slowly reactive to light. Brisk and easily elicited oculocephalic reflexes. Failure to condition to semi-noxious stimuli (e.g. acoustic startle, repetitive glabellar taps). Mild spasticity affected all four limbs and reflex responses to mildly noxious somatic stimuli. Absent P-100 VEP responses bilaterally. Diffuse slowing of EEG. | Expression of single short words, sometimes in small clusters, every 48–96 h. Spontaneous grimace, only weakly evoked by shouts, words, music and noxious stimuli. Episodic chewing, bruxism and saliva swallowing. |

**Table 1** *Continued*

| Patient (sex/age) | Duration of PVS | Clinical history | Clinical examination | Observable behaviour |
|---|---|---|---|---|
| 4 (M/21) | 7 months | Blunt head trauma with subdural and tentorial haematomas. Immediate coma progressing to vegetative state at 6 weeks. | Head and eyes were consistently turned to the left. Passively turning the head to the right elicited tonic leftward eye movements. Full oculocephalic reflexes. Generalized startle myoclonus, failure to condition to eyebrow tapping and no focal responses to noxious stimuli. Sustained flexor posture in all four limbs accentuated by local stimulation. | None except recurrent cyclic arousal with eyes open alternating with eyes closed periods. |
| 5 (M/26) | 6 years | Motor vehicle accident leading to right uncal herniation secondary to right epidural decompressed with a temporal lobectomy. Subdural haematomas and Duret haemorrhage of mesencephalon. | Targetless roving eye movements. Oculocephalic reflexes released without fast components. Right pupil fixed at 4 mm; left pupil responds sluggishly. Posturing to mild exogenous stimuli. Noxious stimuli evoked extensor or flexor postural reflexes, but muscle tone not spastic and muscle bulk relatively preserved. Extensor plantar responses. 24-h EEG demonstrated a diffuse and disorganized low-voltage tracing with slowing in the delta and theta range through all channels during both eyes open and eyes closed periods. | Constant chewing of objects placed in mouth. |

### Patient 2

Patient 2 suffered severe head trauma in a motor vehicle accident followed by a post-operative cardiopulmonary arrest. Seven years of repeated neurobehavioural assessments conducted prior to this study consistently indicated a diagnosis of PVS. Accordingly, Patient 2 showed no evidence of inter-personal contact or awareness of self or environment. He did, however, display selective emotional behavioural responses. When touched or presented with loud noises, he intermittently demonstrated clenched teeth, strong and forced groans, hypertension, tachycardia, facial flushing and pupillary dilatation. The outbursts considerably resembled the sham rage responses observed by Cannon following stimulation in decerebrated cats (Cannon, 1929; see also Panksepp, 1998). Conversely, soft music or a gentle tone of the observer's voice (particularly that of his mother) tended to quiet him, reflecting a partial capacity for the receptive processing of prosody.

MRI identified diffuse supra- and infratentorial atrophy associated with dilated ventricles and wide cerebral sulci. Specific focal atrophic areas included the bilateral calcarine regions as well as the frontal and parietal lobes. Prominent, diffuse leucoencephalopathy involved both occipital areas.

Figure 3A displays the PET data for Patient 2. A right–left asymmetry is apparent with relatively increased metabolic activity in the right hemisphere. Figure 3B shows a histogram of the mean values of metabolic rates as a percentage of normal values for individual brain regions. Resting metabolism was substantially reduced across all brain regions, varying from 20 to 42% of normal resting rCMRglc. Average CMRglc for the brain was 31.46% of normal. The greater rCMRglc of the right hemisphere compared with the left hemisphere (34% versus 28% of normal metabolic rates) confirms the hemispheric asymmetry observed on the PET images. In Fig. 3C, the PET regions expressing >35% of normal rCMRglc are overlaid onto the patient's MRIs. In these images, peak values >45% of normal rCMRglc were observed in the right putamen, caudate nucleus, orbitofrontal cortex, lateral and superior temporal cortex, and bilaterally in medial temporal cortex.

MEG recordings resulted in remaining magnetic fields in response to bilateral auditory stimulation, but only within the right hemisphere. Main peaks were detected at ~80 and 131 ms and localized to the right superior temporal area on the MRI with a 97/98% goodness of fit (Fig. 3D). In addition to an abnormal but dominant lower frequency response, a weak and incomplete time-locked response of gamma band activity restricted to the right hemisphere was observed in response to auditory stimuli. The sequence of temporal activations, while incomplete, nevertheless, clearly localizes to the proximity of right temporal area. This corresponds to islands of relatively preserved metabolism as seen in the patient's PET data (above). The goodness of fit was 95% for dipole localization.

In response to tactile stimulation, abnormal MEFs were detected on the contralateral hemisphere at ~100/140 ms (right hemisphere) and 120/170 ms (left hemisphere). There was also a delay on the left hemisphere in response to right tactile stimuli (Fig. 3E). A partial time-locked response in the gamma band range was also observed in the contralateral hemispheres, concomitant with a larger response on the right hemisphere to left tactile stimuli. Source estimates for lower and higher frequency activations were restricted to contralateral sensorimotor areas of the right hemisphere, with a goodness of fit of 99% for all locations, and displaced to contralateral superior frontal areas of the left hemisphere for both low- and high-frequency activations (Fig. 3E). The goodness of fit for the source estimates on the left hemisphere was 99% for sources in the lower frequency range, and 91–95% for sources in the gamma band.

These MEG data indicate a greater loss and distortion of sensory processing within the left hemisphere and partially preserved, but delayed and incomplete processing within the right hemisphere.
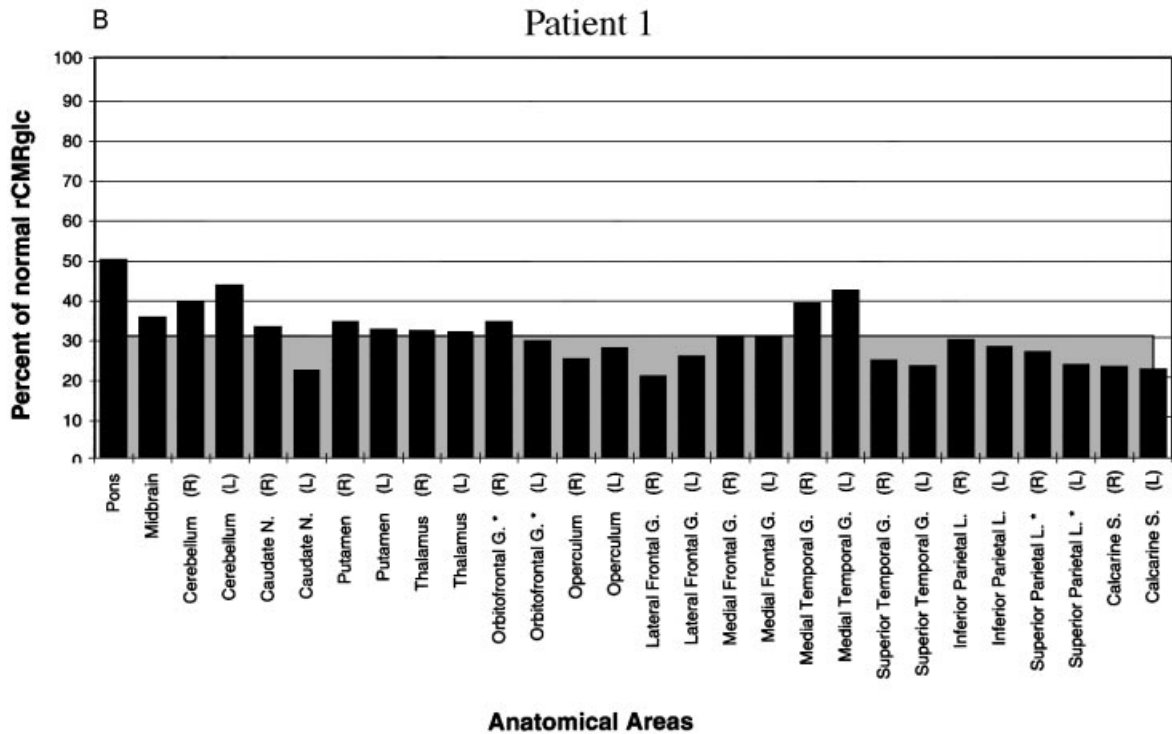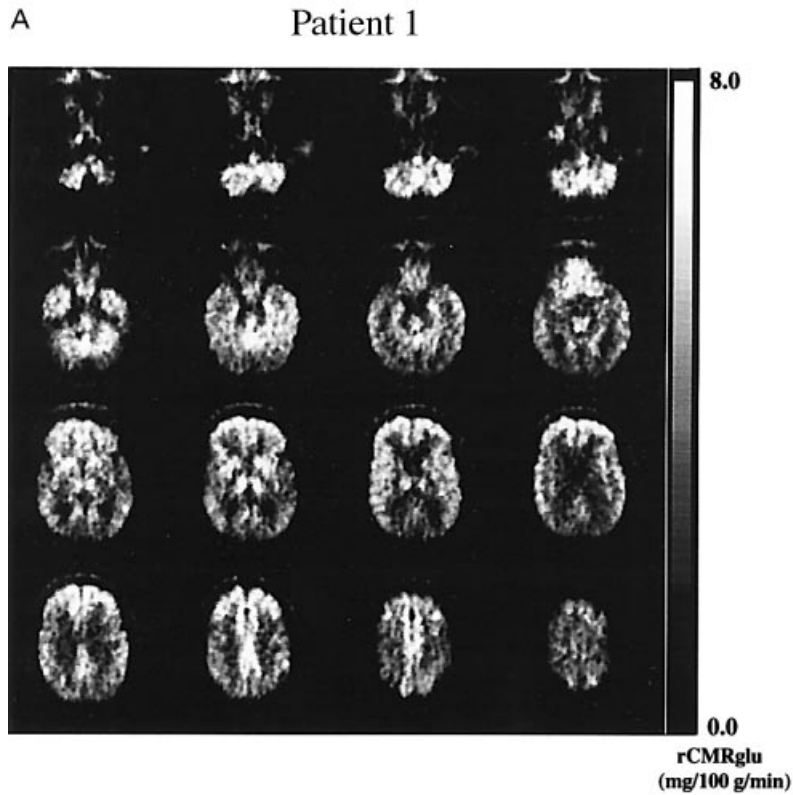
### Interpretation

Patient 2's relatively preserved glucose metabolism in the right temporal–parieto-occipital junction (Fig. 3Ca), right caudate (Fig. 3Cb) and the right pre- and orbitofrontal cortices (Fig. 3Cc) correlates strongly with his displayed explosive rage and responses to prosodic stimuli. These component regions include all of the cortical and subcortical regions that, when injured, may induce aprosodia (Ross, 1997). Similarly, these right hemisphere structures are also implicated in processing of music (Liegeois-Chauvel *et al.*, 1998). We interpret the patient's response of quieting to music or soothing tones of voice to reflect the persistence of a circuit that can process prosody. The sham rage emotional responses of the patient may relate to the connection of this right hemisphere circuitry to the ipsilateral amygdala and hypothalamus (Panksepp, 1998). de Jong *et al.* (1997) used regional cerebral blood flow studies to demonstrate selective activation of an isolated right hemisphere to voice in a child, vegetative for 2 months, and interpreted these findings as possibly reflecting limited prosodic processing. Recently, modular prosodic processing from right hemisphere structures was reported in a patient with global aphasia and extensive left hemisphere injury (Barrett *et al.*, 1999). Our imaging data suggest that a similar, connected and isolated, modular network remains active in Patient 2 and retains the partial capacity to process and react to prosodic stimuli. This conclusion is strengthened by the isolated presence of incompletely expressed auditory evoked responses detected by MEG over the right auditory cortex.

In Patient 2, a time-locked gamma band activity in response to auditory stimulation was localized and restricted to the right temporal area. The AEF components were also restricted to the right hemisphere only within temporal areas. In addition, a temporal sequence of gamma band source activations was incomplete. This activation corresponded to relatively preserved right hemisphere metabolic activity; and

the MEG data provide a strong basis for inferring a partially preserved right hemisphere circuit underlying the patient's responses to prosodic stimuli.

### Patient 3

For >20 years after acute brain damage secondary to successive primary cerebral haemorrhages, Patient 3 has



A    Patient 1

8.0

0.0

rCMRglu
(mg/100 g/min)



B    Patient 1

Percent of normal rCMRglc

Anatomical Areas

Pons, Midbrain, Cerebellum (R), Cerebellum (L), Caudate N. (R), Caudate N. (L), Putamen (R), Putamen (L), Thalamus (R), Thalamus (L), Orbitofrontal G. * (R), Orbitofrontal G. * (L), Operculum (R), Operculum (L), Lateral Frontal G. (R), Lateral Frontal G. (L), Medial Frontal G. (R), Medial Frontal G. (L), Medial Temporal G. (R), Medial Temporal G. (L), Superior Temporal G. (R), Superior Temporal G. (L), Inferior Parietal L. (R), Inferior Parietal L. (L), Superior Parietal L. * (R), Superior Parietal L. * (L), Calcarine S. (R), Calcarine S. (L)

been noted to utter short, understandable, single and irrelevant words sometimes in small clusters at intervals of ~48–96 h (Table 1). Repeated clinical evaluations have provided no evidence of interpersonal interaction or self-awareness as assessed by command following, object pursuit, verbal or gestural communication or other patterned responses.

MRI scans identified severe post-haemorrhagic subcortical damage, including the right cerebral white matter as well as a large posterior temporoparietal region in the left hemisphere. The right thalamus and basal ganglia appeared entirely destroyed, as did the left posterior thalamus.

Figure 4A displays an overview of the PET data obtained in Patient 3. A marked right–left asymmetry is evident, with several areas of relatively preserved glucose metabolism identified in the left hemisphere. Figure 4B shows a histogram of the regional metabolic rates for mean values as a percentage of normal metabolism. The average global

metabolic rate expressed in the brain is 43.77% of normal, with a mean left hemisphere activity of 52% of normal and a mean right hemisphere activity of 32% of normal. Mean metabolic rates greater than the global brain average were observed bilaterally in pons and midbrain, in the left basal ganglia, bilateral orbitofrontal gyri, left frontal operculum, left medial temporal gyrus, left superior temporal gyrus, left inferior and superior parietal cortices and left calcarine cortex.

Figure 4C displays the PET voxels expressing >55% of normal rCMRglc co-registered onto the patient's MRIs. The three slices through the superior temporal sulcus and inferior frontal regions illustrate the highly localized areas of preserved metabolism including the medial and superior temporal gyrus and the frontal operculum. The three slices through the superior temporal sulcus and inferior frontal regions illustrate the highly localized areas of preserved
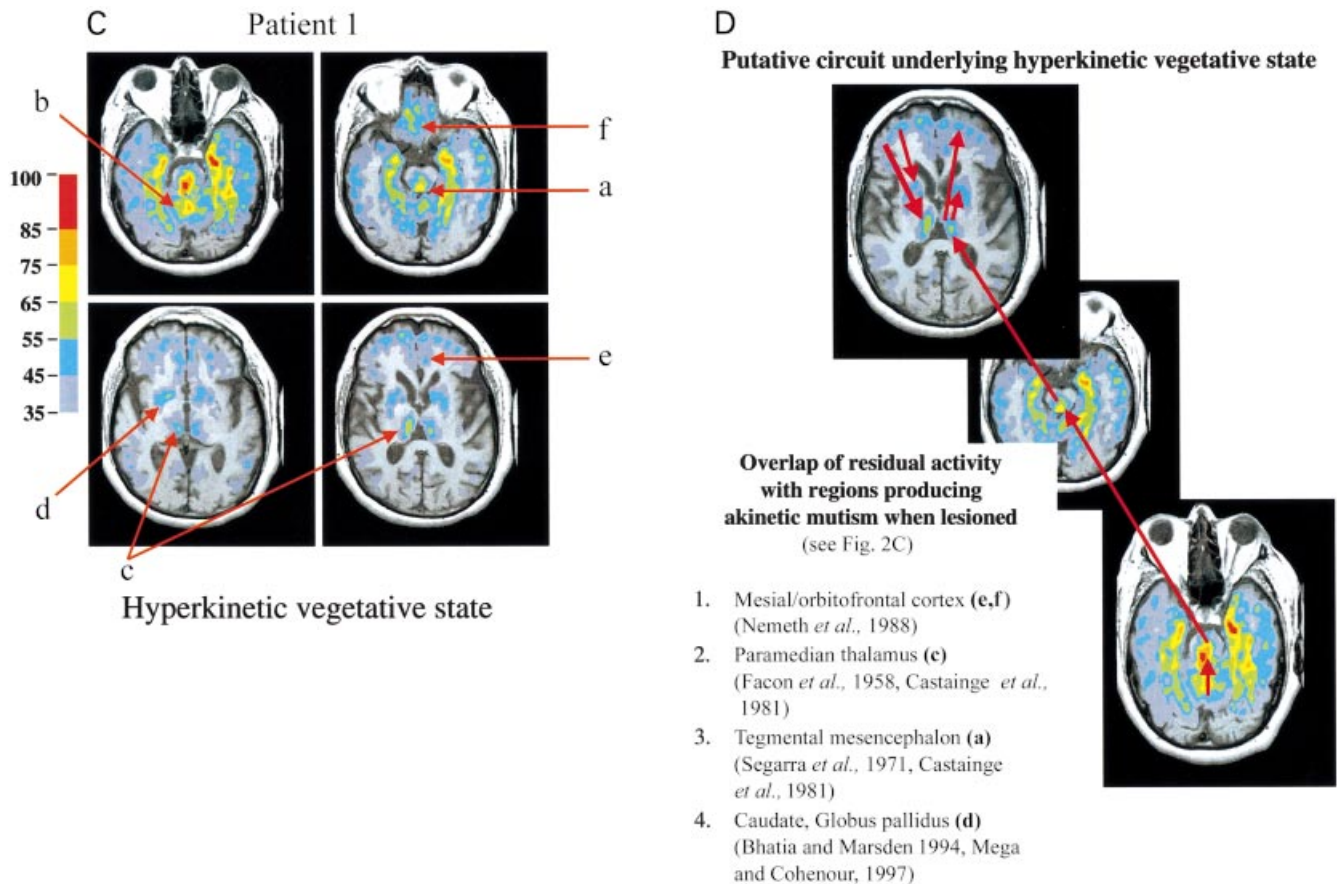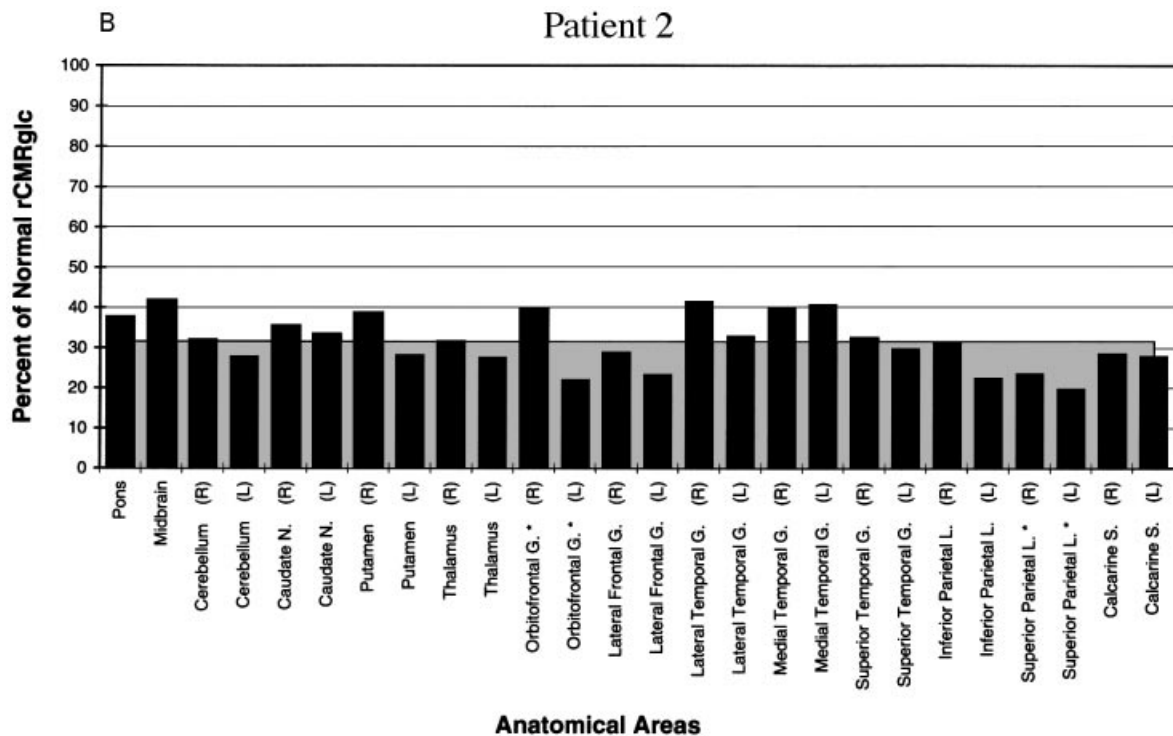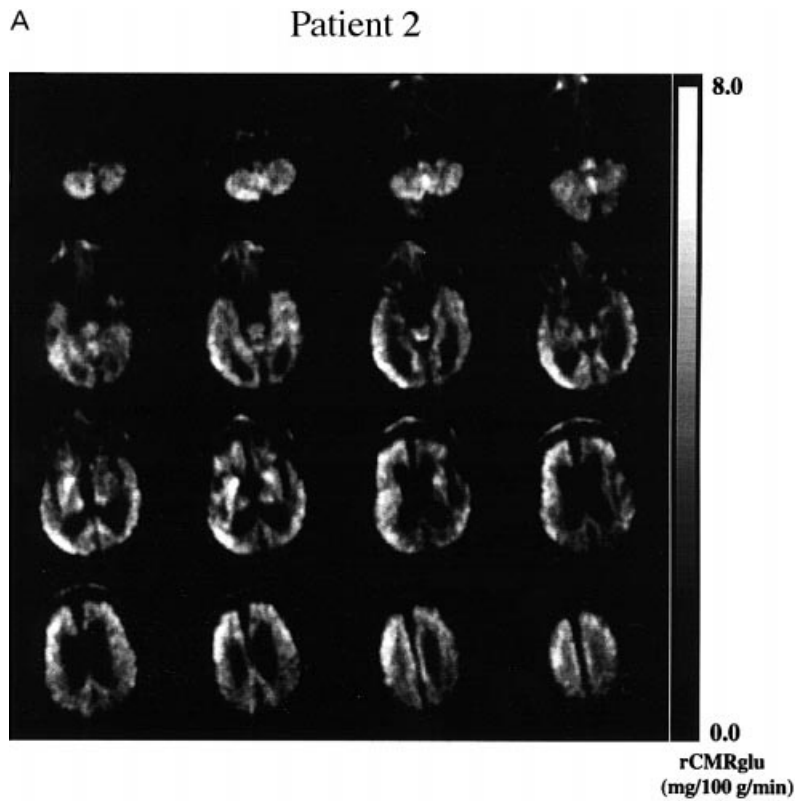


**Fig. 2** (**A**) Raw FDG-PET data for Patient 1 are displayed on an arbitrary grey scale; saturation of brightness corresponds to 8.0 mg/100 g/min of glucose metabolism. Increased metabolic activity is noted in several anterior brain structures (see text). (**B**) Regional cerebral metabolic rates are plotted for individual brain structures (black bars) and the average brain value (grey block) as a percentage of normal values. * = structures for which comparison is among a smaller sample of normal values (see Methods). L = left. R = right. (**C**) Co-registered MRI and PET images are displayed. PET voxels are normalized by region and expressed on a colour scale ranging from 35 to 100% (within the second standard deviation) of normal. Labelled structures: tegmental pons and tegmental mesencephalon (a), cerebellum (b), posterior thalami (c), caudate nuclei (d), prefrontal (e) and orbitofrontal (f) cortices. (**D**) Illustration of overlap of PET voxels (**C**) with residual metabolic activity and structural injuries producing akinetic mutism. Arrows schematically indicate known ascending connections from the brainstem and cerebellum to the thalamus and corticostriatopallidal–thalamocortical loop connections. Descending connections from cortex to brainstem are not diagrammed.

metabolism. These regions of preserved glucose metabolism appear to include Heschl's gyrus and Wernicke's area (Fig. 4Ca), Broca's area (Fig. 4Cb) and the left caudate nucleus (Fig. 4Cc).

Analysis of MEG data indicated intermittent spontaneous gamma band activity restricted to the left hemisphere. Indeed, a sequential spectral analysis, analysed within a time window of 128 ms over a time period of 1 min, clearly demonstrated
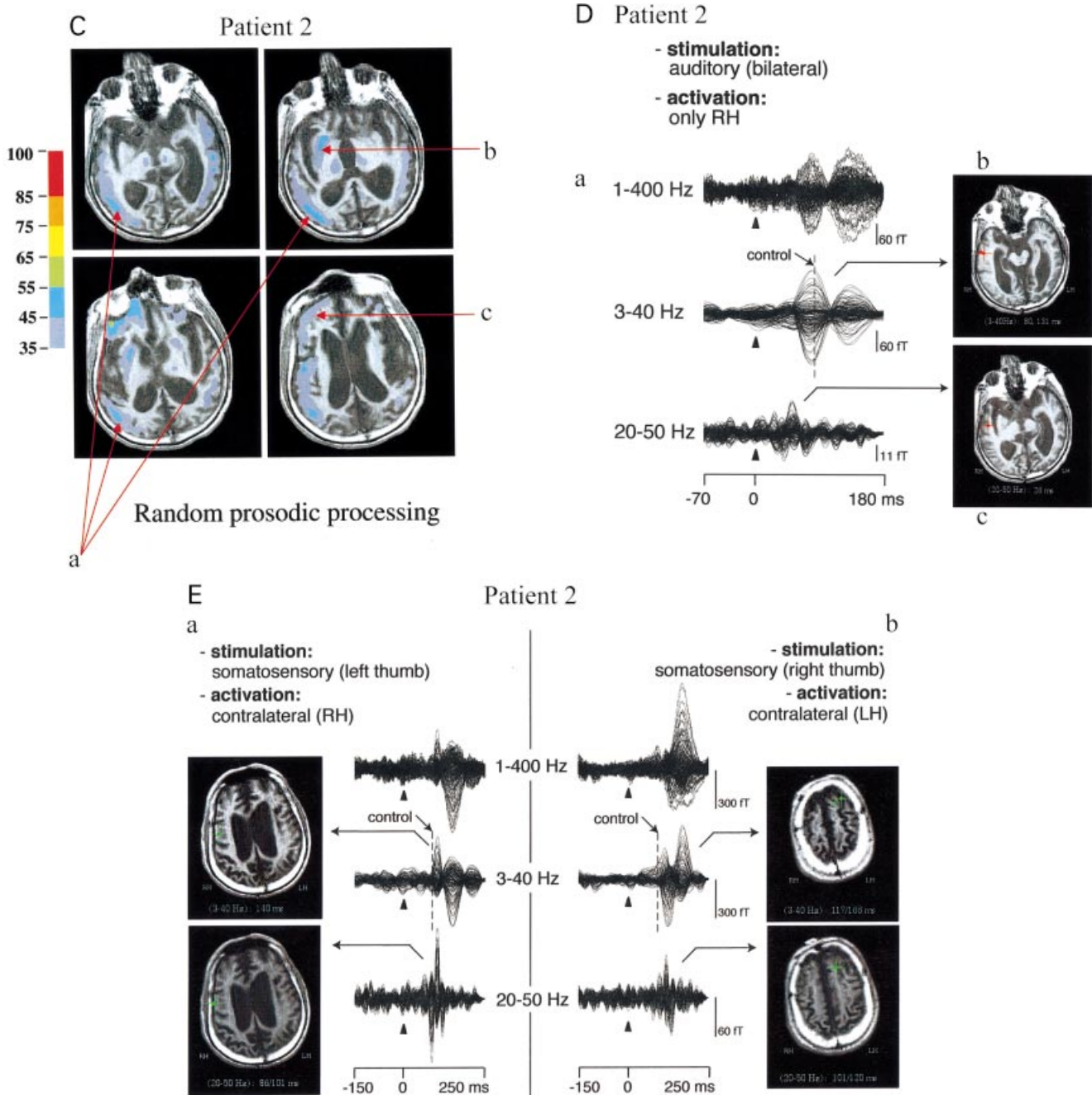
A    Patient 2



rCMRglu
(mg/100 g/min)

B    Patient 2

**Fig. 3** (**A**) Raw FDG-PET data for Patient 2 are displayed on an arbitrary grey scale; saturation of brightness corresponds to 8.0 mg/100 g/min of glucose metabolism. Relatively preserved metabolic activity is noted in right hemisphere structures (see text). (**B**) Regional cerebral metabolic rates are plotted for individual brain structures (black bars) and the average brain value (grey block) as a percentage of normal values. * = structures for which comparison is among a smaller sample of normal values (see Methods). L = left; R = right. (**C**) Co-registered MRI and PET images are displayed. PET voxels are normalized by region and expressed on a colour scale ranging from 35 to 100% (within the second standard deviation) of normal. Labelled structures: right temporal–parieto-occipital junction (a), right caudate (b), and the right pre- and orbitofrontal cortices (c). (**D**) Evoked magnetic fields in response to bilateral auditory stimulation and localization to the right hemisphere only. In (a), averaged waveforms are superimposed for all MEG channels and displayed unfiltered (1–400 Hz), and filtered at 3–40 and 20–50 Hz. (b) AEF components are identified at ~80 and 131 ms, localizing to the right superior temporal area only on the co-registered MRI. Goodness of fit: 97/98%. Dashed line indicates control N100. (c) A weak and incomplete time-locked gamma band activity localizing only to the right temporal area at 26 ms is observed, with a goodness of fit of 95% for the localization. (**E**) Contralateral evoked magnetic fields in response to unilateral tactile stimulation. (a) Right hemisphere activation, left thumb stimulation. Averaged waveforms are superimposed for all MEG channels and displayed unfiltered (1–400 Hz), and filtered at 3–40 and 20–50 Hz. Magnetic evoked field components are seen at ~102 and 140 ms (3–40 Hz; dashed line indicates main deflection in control), localizing within sensorimotor areas. Goodness of fit: 99%. A partial time-locked activity in the gamma band (20–50 Hz) localizes to sensorimotor areas. Goodness of fit: 99%. (b) Left hemisphere activation, right thumb stimulation. Magnetic evoked field components are seen at ~117 and 166 ms (3–40 Hz), localizing to contralateral superior frontal areas. Goodness of fit: 99%. A partial time-locked activity in the gamma band (20–50 Hz) also localizes to contralateral superior frontal areas. Goodness of fit: 91–95%.

some preserved gamma band activity in the left hemisphere (Schiff *et al*., 1999). Time-locked gamma band activity was also observed in the left hemisphere in response to bilateral auditory stimulation. The response, however, was abnormal, reflecting a poorly synchronized waveform compared with the response in normal controls (Joliot *et al*., 1994). Single-dipole analysis localized a dominant but abnormal cortical component of the gamma band activity to the left Heschl's



A    Patient 3

12.0

0.0
**rCMRglu
(mg/100 g/min)**



B    Patient 3

**Anatomical Areas**
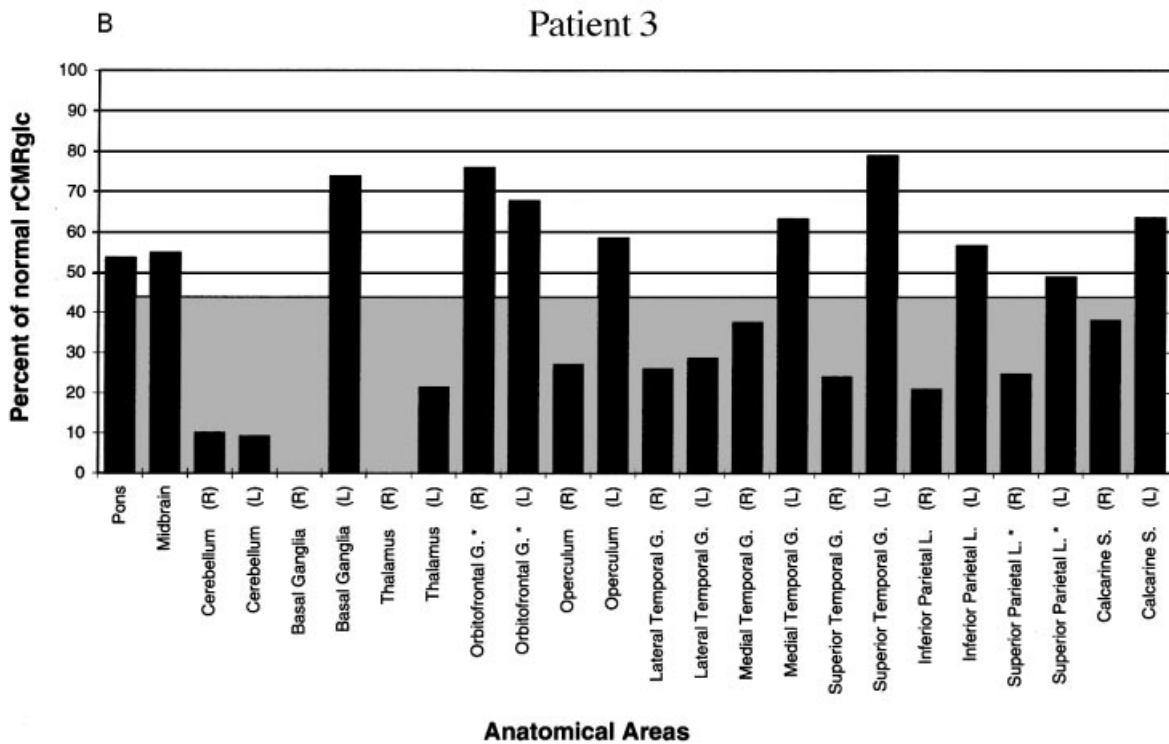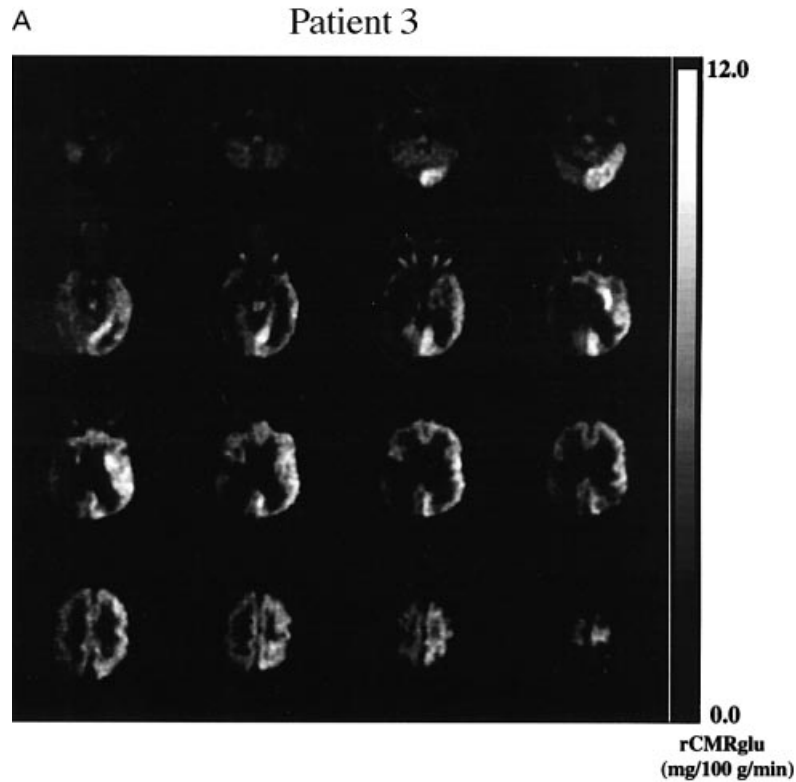
gyrus on the MRI that coincided with the partially preserved metabolically active regions identified by FDG-PET (Schiff *et al.*, 1999).

Single somatosensory stimuli applied to the left index finger induced a weak and incomplete time-locked gamma band activity restricted to the ipsilateral left hemisphere (Fig. 4D) compared with the expected contralateral response in healthy humans. The sequence of activations in Patient 3 was observed initially at the somatosensory cortex and then, during a second peak, at the ipsilateral temporal lobe. While the displacement of the second peak agrees with the partially preserved metabolic imaging results and may be physiologically meaningful, it may also result from the decrease in signal coherence. Nevertheless, the goodness of fit was relatively high (90%) for all localizations. Single-dipole estimates also localized well to areas of relatively increased residuals of brain metabolism identified by PET measurements.

### Interpretation

We previously have discussed the correlation of remnant word expression with anatomical regions, preserved glucose metabolic activity and the presence of gamma band activity restricted to the left hemisphere observed in Patient 3 (Schiff *et al.*, 1999). We interpret the functional preservation of several key anatomical structures of the human language system, Broca's and Wernicke's area and their underlying cortical and subcortical connections, to be a remnant circuit capable of generating isolated words as fixed motor action patterns.

### Patient 4

Seven months prior to our studies, Patient 4 suffered severe head trauma complicated by bilateral subdural haematomas leading to coma. Within a few weeks, he regained vegetative wakefulness, following which he displayed no evidence of awareness, intentional activity or purposeful activity as assessed by command following, object pursuit, verbal or gestural communication or other patterned responses. His behaviour was consistent with the classic description of PVS (Jennett and Plum, 1972; see Table 1).

MRI flare images demonstrated multifocal shear injuries in the subcortical white matter and multiple contusions affecting both frontal and temporal lobes. Gradient echo imaging identified marked damage to the posterior splenium of the corpus callosum.

Figure 5A shows the PET data for Patient 4. Several right and left hemisphere regions appear as islands of relatively
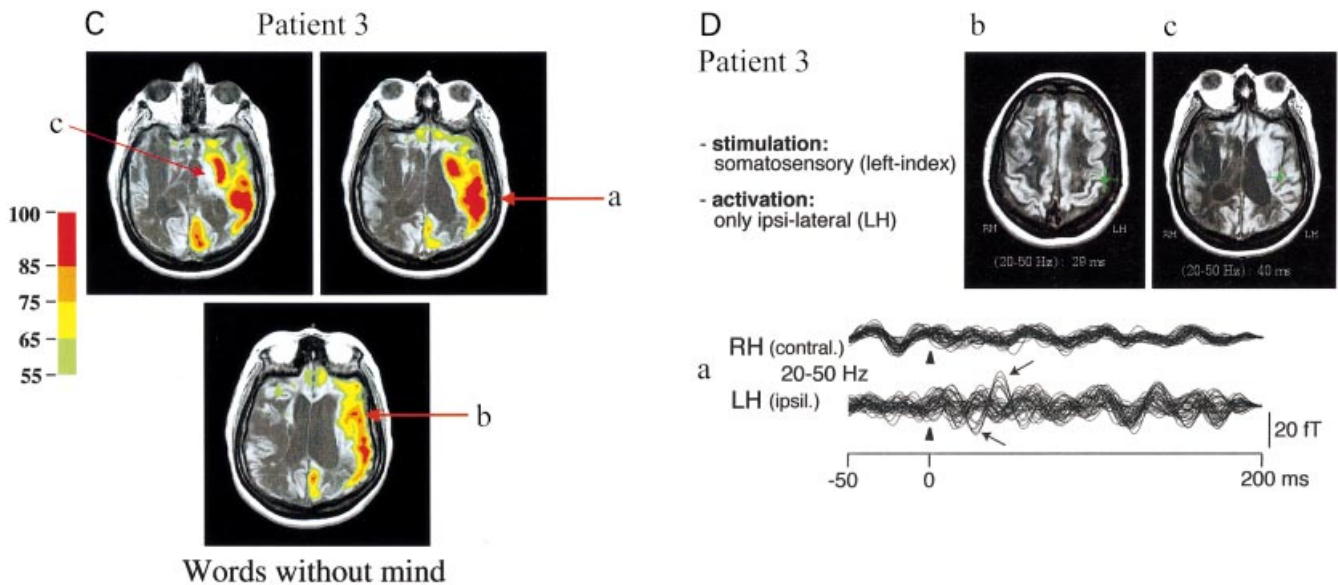


**Fig. 4** (**A**) Raw FDG-PET data for Patient 3 are displayed on an arbitrary grey scale; saturation of brightness corresponds to 12.0 mg/100 g/min of glucose metabolism. Note the change from plots of Patients 1 and 2 (Figs 2A and 3A). Relatively preserved metabolic activity is noted in left hemisphere structures (see text). (**B**) Regional cerebral metabolic rates are plotted for individual brain structures (black bars) and the average brain value (grey block) as a percentage of normal values. * = structures for which comparison is among a smaller sample of normal values (see Methods). L = left; R = right. (**C**) Co-registered MRI and PET images are displayed. PET voxels are normalized by region and expressed on a colour scale ranging from 55 to 100% (within the second standard deviation) of normal. Labelled structures: Heschl's gyrus and Wernicke's area (a), Broca's area (b) and the left caudate nucleus (c). (**D**) (a) A weak and incomplete time-locked gamma band activity (20–50 Hz) restricted to the ipsilateral left hemisphere only (see arrows) is present in response to somatosensory stimuli applied to the left index finger. The temporal sequence of gamma band activations localizes first (29 ms) to the proximity of ipsilateral sensory areas (b) and then, during a second peak (40 ms), to ipsilateral temporal areas (c). The goodness of fit for single dipole analysis was 90% for all localizations. Note the dislocation in space (ipsilateral hemisphere) and in the temporal sequence.

preserved metabolism surrounded by a largely homogenous background of lower metabolic expression. Figure 5B shows a histogram of the mean metabolic rates for each brain structure as a percentage of normal values. The average brain CMRglc is 55% of normal. Areas expressing greater than average metabolic rates included the pons, midbrain, right

A    Patient 4



rCMRglu
(mg/100 g/min)

B    Patient 4



**Anatomical Areas**
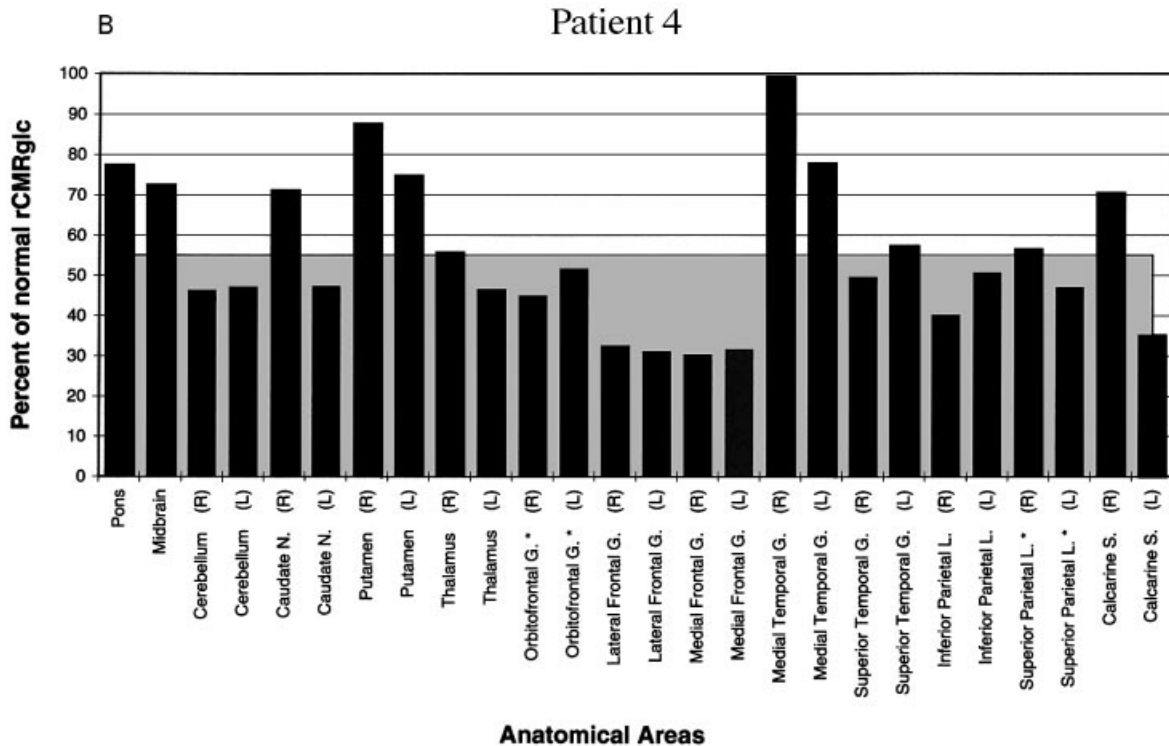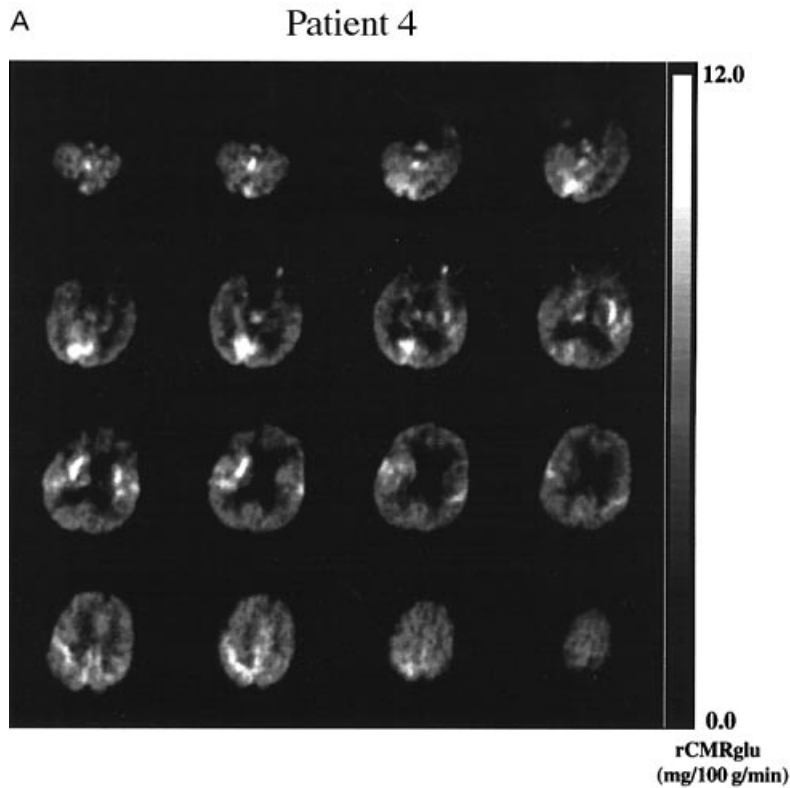
caudate nucleus, right and left putamen, right thalamus, right and left medial temporal gyri, left superior temporal gyrus, right superior parietal lobule and right calcarine region. Figure 5C shows the PET regions that express >55% of normal rCMRglc co-registered onto the patient's MRIs.

MEG recordings in this patient demonstrated a unique finding of loss of high-frequency gamma band activity despite preservation of a low-frequency network response to sensory stimuli. In response to unilateral tactile stimuli, primary evoked magnetic fields (SEFs) demonstrated weak and
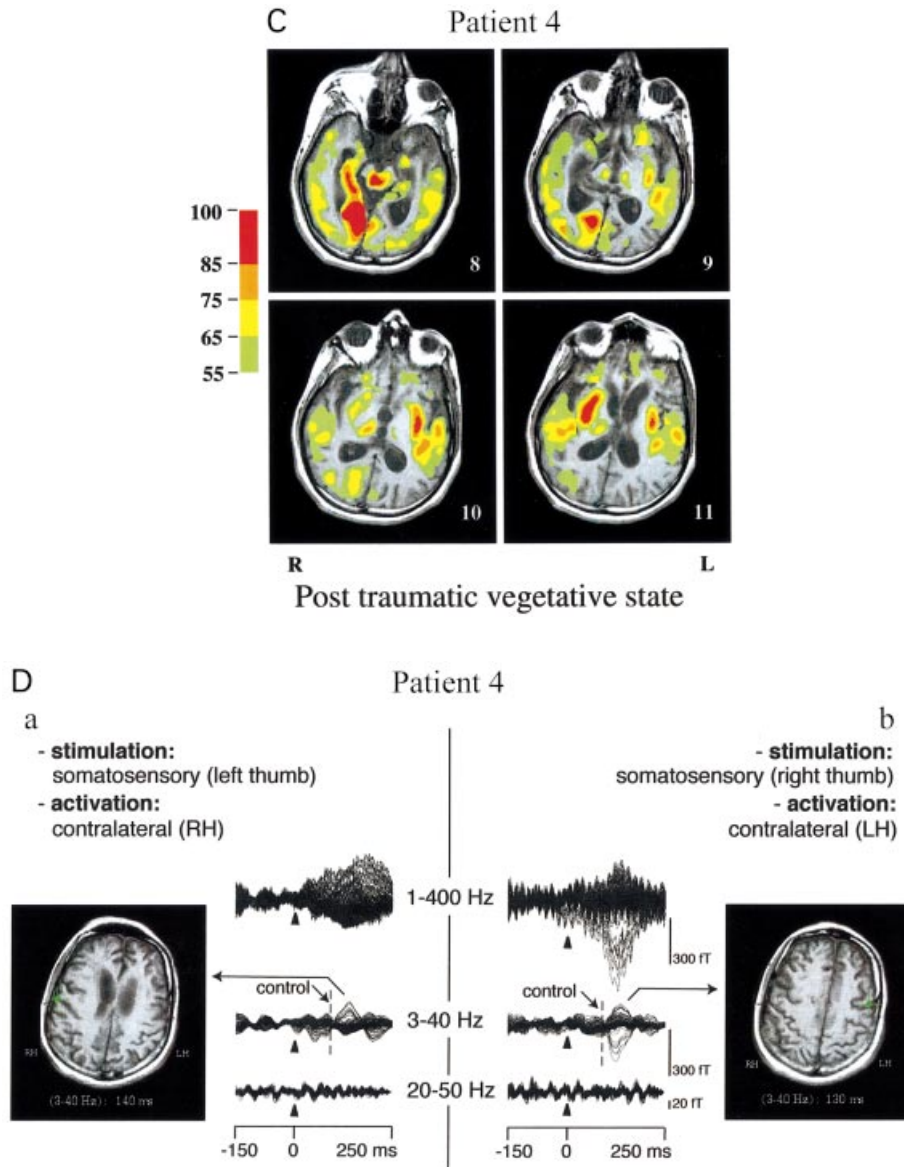


**Fig. 5** (**A**) Raw FDG-PET data for Patient 4 are displayed on an arbitrary grey scale; saturation of brightness corresponds to 12.0 mg/100 g/min of glucose metabolism. Note the change from plots of Patients 1 and 2 (Figs 2A and 3A). Relatively preserved metabolic activity is noted in right posterior occipital and basal ganglia structures (see text). (**B**) Regional cerebral metabolic rates are plotted for individual brain structures (black bars) and the average brain value (grey block) as a percentage of normal values. * = structures for which comparison is among a smaller sample of normal values (see Methods). L = left; R = right. (**C**) Co-registered MRI and PET images are displayed. PET voxels are normalized by region and expressed on a colour scale ranging from 55 to 100% (within the second standard deviation) of normal. (**D**) Contralateral somatosensory evoked magnetic fields (SEFs) demonstrate a lack of time-locked activity in the gamma band. (a) Right hemisphere activation, left thumb stimulation. Averaged waveforms are superimposed for all MEG channels and diplayed unfiltered (1–400 Hz), and filtered at 3–40 and 20–50 Hz. The magnetic evoked field component is seen at ~140 ms (3–40 Hz; dashed line indicates main deflection in control), localizing within sensorimotor areas. Goodness of fit: 99%. There is no evidence of time-locked activity in the gamma band (20–50 Hz). (b) Left hemisphere activation, right thumb stimulation. Averaged waveforms are superimposed for all MEG channels and diplayed unfiltered (1–400 Hz), and filtered at 3–40 and 20–50 Hz. The magnetic evoked field component is seen at ~130 ms (3–40 Hz), localizing within sensorimotor areas. Goodness of fit: 96%. There is no evidence of time-locked activity in the gamma band (20–50 Hz).

delayed contralateral brain activations at ~30 and 140 ms for the left and right hemisphere, respectively, in the proximity of sensorimotor areas. Somatosensory responses to bilateral stimuli with a goodness of fit of 96–99% for the left/right hemisphere are shown in Fig. 5D.

*Interpretation*

Despite the fact that Patient 4 demonstrated several small islands of relatively preserved metabolism, he expressed no behavioural fragments. Without a behavioural correlation, it is difficult to infer any relevant function of the group of



A    Patient 5

rCMRglu
(mg/100 g/min)



B    Patient 5

Percent of normal rCMRglc

Anatomical Areas
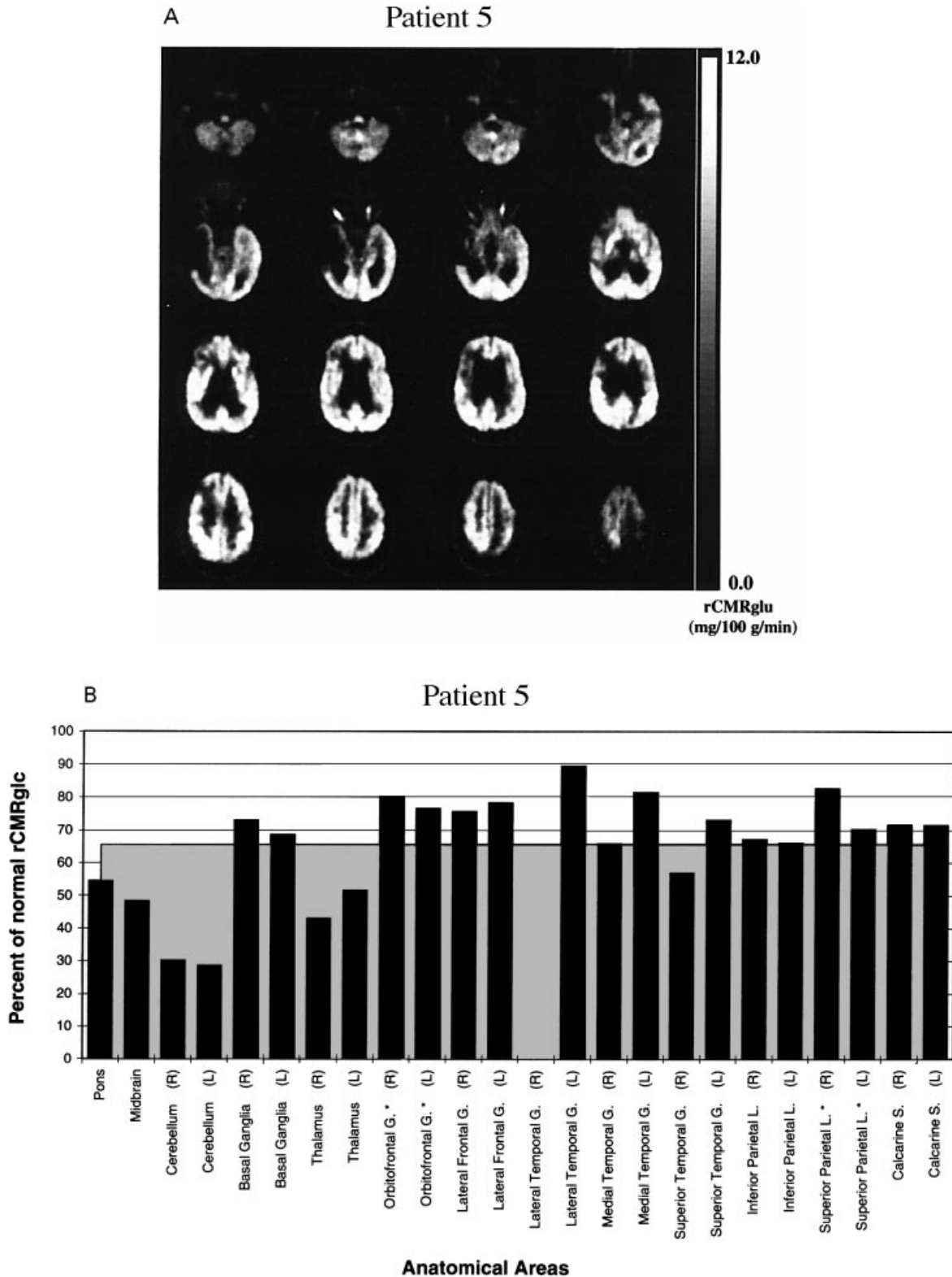
observed structures. However, the coincident preservation of metabolism in several brain regions in Patient 4 may indicate that these regions represent silent, but partially functional sensory circuits. Of note, a recently published [$^{15}$O]PET study (Menon *et al.*, 1998) reported activation of such clinically silent posterior cerebral regions in a patient during a PVS of short duration. The bilateral loss of high-frequency activity in this patient may also reflect the role of feedback from motor regions in this response (Ribary *et al.*, 1999). This patient suffered severe injuries to both motor cortices as evidenced by profound spasticity on clinical exam.

### Patient 5

Six years prior to our study, Patient 5 suffered acute trauma leading to right epidural haematoma and a subsequent Duret haemorrhage secondary to severe uncal and caudal transtentorial herniation (Table 1). His behaviour fits the classic
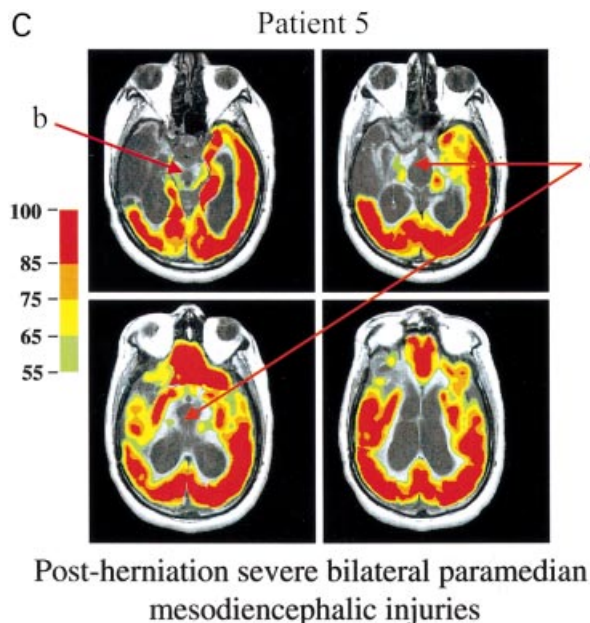


Post-herniation severe bilateral paramedian mesodiencephalic injuries

**Fig. 6** (**A**) Raw FDG-PET data for Patient 5 are displayed on an arbitrary grey scale; saturation of brightness corresponds to 12.0 mg/100 g/min of glucose metabolism. Note the change from plots of Patients 1 and 2 (Figs 2A and 3A). Highly preserved cortical activity is noted compared with Patients 1–4. The paramedian mesodiencephalic region shows marked reductions of metabolic activity (see text). (**B**) Regional cerebral metabolic rates are plotted for individual brain structures (black bars) and the average brain value (grey block) as a percentage of normal values. * = structures for which comparison is among a smaller sample of normal values (see Methods). L = left; R = right. (**C**) Co-registered MRI and PET images are displayed. PET voxels are normalized by region and expressed on a colour scale ranging from 55 to 100% (within the second standard deviation) of normal. Labelled regions: medial thalamus (a) and tegmental mesencephalon (b).

patterns of PVS with no response to command, localization of stimuli or evidence of communication (Jennett and Plum, 1972). MRI revealed marked cortical atrophy as well as diffuse white matter abnormalities and abnormal signal intensities in the left parietal cortex and basal ganglia. Haemosiderin deposits in the midbrain identified an earlier mesencephalic haemorrhage at the level of the superior colliculi. Severe, diffuse atrophy affected the brainstem along with paramedian thalamic atrophy accompanied by wide dilation of the third ventricle. Continuous video-EEG recordings demonstrated low-frequency, low-amplitude activity without change during eyes open or eyes closed periods. There was no evidence of a sleep/wake architecture.

Figure 6A displays Patient 5's PET data. The data are remarkable for showing a high degree of cortical and subcortical activity. Conversely, the paramedian mesodiencephalic structures demonstrate severely reduced glucose metabolism. Figure 6B shows a histogram of mean values expressed as percentages of normal. The average CMR for Patient 5's brain was 65.45% of normal. More cortical structures showed metabolic activity above the average, while pons, midbrain, cerebellum and thalamus showed activity below average. The lowest activity was observed in the mesencephalon and thalamus. In the mesencephalon, the only detectable metabolic signal was restricted to the lateral rim of the structure. The thalamus similarly appears atrophic (note the enlarged third ventricle) with some preserved metabolic activity.

Figure 6C illustrates the PET voxels expressing >55% of normal rCMRglc co-registered onto the patient's MRIs. Note the remarkable preservation of metabolism in the atrophied cortex of this man compared with the previous four patients.

### Interpretation

The unexpected results of Patient 5's FDG-PET study showing a near-normal cortical metabolic rate, but severely damaged medial thalamus and mesencephalon demonstrate the selective and indispensable contribution of these paramedian circuits to generating conscious awareness. Amplifying this known clinical–pathological correlation, however, the PET data illustrate an unsuspected, relative preservation of cortical metabolism co-existing in a cerebrum deprived of its integrative thalamocortical cognitive capacities (see Discussion for further interpretation).

## Discussion
### FDG-PET imaging of the persistent vegetative state

Functional neuroimaging studies of severely damaged brains present a significant challenge for using standard techniques. As demonstrated above, patients with complex brain injuries may suffer distortions of normal neuroanatomy secondary to atrophy and loss of both grey and white matter structures. As

a result, their brains often cannot be mapped accurately into available reference atlases or easily presented in standard sections. Careful PET/MRI co-registration and individual patient analysis, however, can overcome some of these problems and allow the identification of important clinical–pathological correlations.

Resting cerebral metabolism derived from quantitative glucose uptake provides an indirect assessment of neuronal activity against which brain states may be compared quantitatively (Levy *et al.*, 1987). As noted above, all previous quantitative FDG-PET investigations of PVS have correlated the condition with a global reduction of brain metabolic activity (Levy *et al.*, 1987; DeVolder *et al.*, 1990; Tommasino *et al.*, 1995; Laureys *et al.*, 1999; Rudolf *et al.*, 1999). In these studies, awake vegetative patients have been recorded as expressing an average cerebral metabolism of ~50% of normal or less, comparable with that found in normal subjects undergoing deep anaesthesia (Blacklock *et al.*, 1987) and well below average normal metabolic rates seen in stage IV sleep (Maquet *et al.*, 1990). These analyses have supported the clinical interpretation of wakeful unconsciousness in the vegetative state (Jennett and Plum, 1972). Most vegetative states result from either post-anoxic or traumatic brain injuries (Multi-Society Task Force on PVS, 1994). Among the entirety, however, only a relatively few patients with post-traumatic injury have been studied with FDG-PET. Tommasino *et al.* (1995) noted wider individual ranges of residual metabolism in post-traumatic vegetative patients than in patients with post-anoxic injuries. Nevertheless, the average metabolism in their patients was also <50% of normal. In our study, patients who had suffered traumatic brain injury without global anoxia or hypoxia (Patients 3–5) demonstrated average resting metabolic rates in selected cerebral structures significantly higher than 50% of normal. Only Patient 5, however, exhibited a resting global metabolic rate of >50% of normal.

Our findings must be put in the context of severely injured, atrophied brains that probably possess highly reduced cortical and subcortical neuronal populations. Thus estimates of percentage of normal activity may be affected by partial volume distortions due to atrophy of brain structures that may downwardly bias estimates of metabolic rates in smaller regions of active neurones contained within our ROIs. Given the large deviations of sample values from normal average values, however, this is unlikely to alter substantively our interpretations of these data. Our findings also differ from previous reports because of the use of careful MRI co-registration and improved PET scanner resolution. Both tools considerably aided the anatomic precision in identifying the abnormal findings and interpretations of the measured PET activity in terms of behavioural–pathological correlation. It is important to note, however, that the regional variations identified are seen in the raw PET data as illustrated above; the thresholding and co-registration procedures employed simply delineate the anatomical localization more clearly.

## MEG imaging of the persistent vegetative state

The MEG data obtained from this set of vegetative patients indicate partially preserved but delayed and abnormally incomplete coherent dynamic brain activity. Taken together with the other functional brain imaging studies and clinical evaluations, the findings indicate the existence of isolated areas which retain anatomical integrity and remain active in modular fashion that can support isolated but defined behavioural events. In the patients studied here, the classical MEF components, identified in normal subjects in response to auditory (Reite *et al.*, 1982; Romani *et al.*, 1982; Pantev *et al.*, 1988, 1989; Yamamoto *et al.*, 1988; Regan, 1989) or somatosensory stimulation (Hari *et al.*, 1984; Okada *et al.*, 1984; Sutherling *et al.*, 1988; Wood *et al.*, 1988; Suk *et al.*, 1991; Mogilner *et al.*, 1993; Nakamura *et al.*, 1998), were either absent, delayed or incomplete compared with responses elicited from healthy controls. Selective disappearance of sensory midlatency responses and early evoked potentials has been reported previously in comatose patients (Pfurtscheller *et al.*, 1983).

Our analysis of the spatiotemporal sequence of higher frequency activations (gamma band activity) revealed abnormal sequences of source activations in magnitude (down to total absence), location and organization. In Patients 2 and 3, a modular fraction of gamma band activity remained partially intact, and correlated in both patients with network connections inferred on the basis of behavioural fragments and anatomic and metabolic data. In Patient 2, an abnormal but relatively complete and stable sequence of activation within right sensorimotor areas in response to left tactile stimulation was also observed. In Patient 3, an abnormal sequence of gamma band activation was present in response to tactile stimulation. While a partial time-locked activity was observed in the ipsilateral hemisphere, there was an additional displacement over time from sensorimotor areas to temporal areas. These findings indicate marked plastic changes associated with long-term abnormal brain function. They suggest possible interaction between somatosensory and auditory modalities, as a result of reorganization.

An abnormal and incomplete sequence of gamma band source activations was observed in all patients except Patient 2, who indicated an abnormal but more complete and relatively stable sequence of activation within right sensorimotor areas in response to left tactile stimulation. Alteration and disappearance of human gamma band activity have also been reported in comatose patients (Firsching *et al.*, 1987), during anaesthesia (Madler *et al.*, 1991) and following brain lesions (Spydell *et al.*, 1985). These findings are consistent with these previous observations, and suggest a partial or complete disconnection of global thalamocortical networks with some partially preserved connections that form isolated networks in PVS patients.

Llinás and Ribary (1993) have proposed elsewhere that consciousness may arise by the resonant gamma band co-activation of thalamocortical-specific and non-specific loops.

This would temporarily conjoin cerebral cortical sites specifically activated at gamma band frequency (Llinás *et al.*, 1998*a*). In this manner, the specific system would provide the content, and the non-specific system would provide the temporal binding of such contents into a single cognitive experience. Indeed, spatiotemporal patterns of gamma band activity directly correlate with sensory perception (Joliot *et al.*, 1994; Sauvé *et al.*, 1998), whereas alterations of this pattern correlate with altered perception. This has been observed in language-based learning disabilities and reflects dysrhythmia and dyschronia within thalamocortical systems (Llinás *et al.*, 1998*b*; Ribary *et al.*, 1999). Recent MEG studies provide evidence that a chronic dysrhythmia within thalamocortical systems at theta band frequency (Llinás *et al.*, 1999) can be observed in several neurological and psychiatric patients. This dysrhythmia may result in abnormal gamma band activity (the 'edge' effect; Llinás *et al.*, 1999) that generates the positive symptoms in those patients (Jeanmonod *et al.*, 1996). Our findings in PVS patients suggest that this condition results from overwhelming disconnection of thalamocortical networks. This view leaves open the interesting possibility that preserved modular fractions of gamma band activity could remain, as seen in Patients 2 and 3. If so, it would imply that isolated modular activation in chronic unconsciousness can support isolated behavioural responses (Plum *et al.*, 1998; Schiff *et al.*, 1999). The findings support the view that normal brain function requires intact specific and non-specific thalamocortical systems to organize local and global patterns of synchronization (McCormick, 1991; Llinás and Ribary, 1993; Contreras *et al.*, 1996; Steriade *et al.*, 1996, 1998). In particular, the MEG studies suggest the necessity of locally synchronized gamma band activity within larger coherent spatiotemporal sequences of brain activations that are reset with sensory input (Ribary *et al.*, 1991; Joliot *et al.*, 1994).

## *Modular brain function accompanying chronic unconsciousness*

The evidence for the apparent existence of isolated remnants of functional brain networks in permanently unconscious patients is novel and invites further interpretation. As classically defined, PVS reflects the uniform and chronic loss of expression of forebrain function (Jennett and Plum, 1972). Patients 1–3 described here, however, demonstrate that wakeful behavioural unawareness as seen in the vegetative states can co-exist with complex behavioural fragments. We propose that the observed behaviours are supported by partially preserved, isolated brain networks that are embedded in (or primarily organized by) the brain regions that retained relatively preserved glucose metabolic rates. We further propose that such preserved brain activity reflects novel evidence for the modular nature of functional networks that underlie normal brain function. Unlike Patients 1–3, Patients 4 and 5 show the absence of behaviour in the

presence of many brain regions with high glucose metabolic rate. These two patients illustrate two different points. Whereas Patient 4 retains islands of activity, his clinical examination demonstrated severe spasticity, thus limiting the expression of possible behavioural fragments. Moreover, the likelihood that preserved posterior sensory cortices may not reveal behavioural correlates is borne out in recent studies of other vegetative patients (Menon *et al.*, 1998; Owen *et al.*, 1999). The lack of behaviour despite widely preserved metabolic activity in the atrophic cortex of Patient 5 is discussed below.

The findings in Patients 1–3 led us to conclude that the observed isolated behavioural expressions indicate both retained synaptic efficacy and functional expression in isolated brain regions expressing relatively preserved metabolic activity. The groups of brain regions identified in Patients 1–3 by FDG-PET appear to contain isolated loops of defined circuitry that include the cerebral cortex, basal ganglia and thalamus. Such segregated, parallel, and relatively isolated corticostriatopallidal–thalamocortical or corticothalamic loops have been proposed on the basis of strong anatomical and physiological evidence (Alexander *et al.*, 1986, 1990). The clinical–pathological inference of preserved functional loop activity despite overwhelming brain injury in these patients supports the concept that these parallel and relatively segregated CSPTC loops may underlie forebrain functional networks. The combination of structural–metabolic imaging and physiological studies with MEG further confirms the presence of partially functional networks (see above) and supports the interpretation of preserved CSPTC loop function.

## *Injuries to paramedian mesodiencephalic structures may produce permanent unconsciousness*

Relatively discrete damage to paramedian brainstem and diencephalic structures (Facon *et al.*, 1958; Plum and Posner, 1980; Castaigne *et al.*, 1981) can selectively cause PVS. Although rare, focal injuries producing sustained vegetative states result only from long rostrocaudal lesions that involve the paramedian brainstem bilaterally and almost invariably include part or all of the paramedian thalamus (Plum, 1991). Autopsy evidence in vegetative patients has identified an anatomic dissociation between a relatively normal cerebral cortex and a severely damaged thalamus (Relkin *et al.*, 1990; Kinney *et al.*, 1994; Adams *et al.*, 2000). Kinney *et al.* (1994) presented pathological data to demonstrate selective paramedian thalamic injuries in one patient in a PVS. This patient, however, had suffered a cardiac arrest and loss of fibres in the corpus callosum, cerebral atrophy and other areas of anoxic cortical injury, making these conclusions less certain. Recently, Jennett and colleagues reported a large series of autopsies of patients in a PVS following acute brain injuries (Adams *et al.*, 2000). They conclude that the common

structural injuries underlying PVS include profound white matter damage and/or thalamic injury. Of note, a structurally normal cerebral cortex, cerebellum and brainstem were identified in some patients suffering either anoxic or trauma injuries.

We know of no functional studies that previously have correlated brain glucose metabolism with extensive bilateral paramedian mesodiencephalic injuries associated with PVS. The results of Patient 5's FDG-PET study show a near-normal cortical metabolic rate but severely damaged medial thalamus and mesencephalon. This finding somewhat resembles an earlier observation by Ingvar and Sourander (1970) who studied a patient with a sharply edged, extensive paramedian mesencephalic injury leading to permanent unconsciousness. They biopsied cortical tissue at 18 months that showed early evidence of loss of cortical neurones without gliosis. At autopsy, significant further loss of cortical neurones was identified.

Accordingly, the fundamental role of the mesodiencephalic systems and the preserved cortical metabolism of Patient 5 deserve further consideration. Moruzzi and Magoun (1949) considered the paramedian tegmental mesencephalon along with the paramedian thalamus (primarily the intralaminar nuclear complex, ILN) to underpin arousal mechanisms. A bisynaptic pathway in the intralaminar nuclei relaying signals from the midbrain reticular core to the cerebral cortex has been demonstrated by physiological activation of individual neurones (Steriade and Glenn, 1982). Detailed investigations have since shown that arousal mechanisms can be generated from many separate brainstem and basal forebrain neuronal populations that widely innervate the cerebral cortex and thalamus (Steriade and Llinás, 1988). Damage to the mesencephalic reticular formation must include fibres of passage from deeper brainstem cholinergic arousal system nuclei (pedunculopontine and lateral dorsal tegmental nuclei), noradrenergic afferents originating in the locus coeruleus, and other afferents that strongly innervate the paramedian thalamus (Marrocco *et al.*, 1994). Thus, an initial arousal deficit must accompany either severe paramedian mesodiencephalic injuries alone or injuries that only damage the paramedian structures of the thalamus. Acute dysfunction that selectively involves the paramedian thalamus alone is heralded by coma (Castaigne *et al.*, 1981). In such cases, however, the coma typically is exceedingly brief and followed by vegetative or akinetic mute states, which may give way to further recovery (Schiff and Plum, 1999). The hallmark of the vegetative state is the recovery of cyclical but irregular arousal, indicating at least a partial recovery of these systems.

The mesencephalic reticular formation, intralaminar thalamic nuclei and reticular nucleus of the thalamus play critical roles in selective cortical activation and attention (Kinomura *et al.*, 1996; Steriade, 1997). Llinás and colleagues have proposed that the intralaminar nuclei support a global information binding process in conjunction with the specific relay nuclei through a thalamocortical resonance mechanism

(Llinás and Pare, 1991; Ribary *et al.*, 1991; Llinás *et al.*, 1994, 1998). The ILN are also proposed to selectively gate CSPTC loops (Groenewegen and Berendse, 1994) and generate transient activations that facilitate specific long-range cortico-cortical connections (Purpura and Schiff, 1997).

Taken together, we conclude that the severely damaged bilateral mesencephalic reticular formation and paramedian thalamic (intralaminar and allied nuclei) injuries in Patient 5 have led to a lack of integration of presumably widely preserved, albeit damaged, cerebral networks. The grossly preserved cortical glucose metabolism found in this patient supports a view that consciousness in the human brain is interdependent upon ascending arousal fibres from several brainstem nuclei combining with closely allied pathways interconnecting the tegmental mesencephalon and paramedian thalamus. These later systems probably provide more selective, integrative inputs to segregated and parallel networks that organize cerebral cortical pathways. In this patient, the disproportionate preservation of glucose metabolism (compared within the group and across all previously studied vegetative patients) suggests that many isolated modules, as suggested in Patients 1–3, co-exist but cannot organize into meaningful patterns of sensorimotor integration. In all five patients studied, a behavioural unconsciousness remained despite evidence of either isolated networks (Patients 1–3) or relatively isolated cortical (Patient 5) or subcortical metabolic activity (Patient 4). The findings support the view that consciousness *per se* requires intact corticothalamic systems (Llinás and Ribary, 1998; Steriade, 2000).

## Functional outcomes and mechanisms underlying severe brain injuries

These observations of partially preserved cerebral activity in chronic PVS patients provide evidence that at least some partially functional cerebral regions can remain in catastrophically injured brains. Whereas PVS patients remain behaviourally unconscious, patients in other conditions such as the minimally conscious state (MCS) may exhibit reliable but inconsistent interaction with their environment (Giacino *et al.*, 2002). Functional neuroimaging comparisons of MCS and PVS patients have not been reported. As evidence for conscious awareness is always indirectly inferred from behaviour, further investigations of brain function in patients rising above a vegetative level will be an important next step. A recent pathological comparison of the vegetative state and patients with severe disabilities, however, demonstrates several important findings in light of our functional studies in PVS. Jennett *et al.* (2001) report 65 autopsies of patients with traumatic brain injury leading either to a vegetative state ($n = 35$) or to severe disability, including MCS patients ($n = 30$). Over half of the severely disabled group demonstrated only focal brain injures, without diffuse axonal injury

or thalamic injury. These findings suggest that significant variations in both underlying mechanisms of cognitive disabilities and residual brain function accompany these severe but less disabling brain injuries.

The unexpectedly wide variations of resting cerebral metabolism accompanying the vegetative state in these five patients suggest a need for greater diagnostic clarity in assessing survivors of severe brain injury. Future additional diagnostic imaging will not alter the potential for functional recovery in chronic vegetative patients. However, identification of less severely brain-injured patients (as measured by outcome), with relatively high degrees of preserved metabolic activity and focal injury patterns, may allow risk stratification for rational interventions (Fins, 2000; Schiff *et al.*, 2000). The rapidly evolving field of cognitive neuroscience and the recent development of therapeutic interventions that target modular networks (Benabid *et al.*, 1993) may improve the possibilities of improving the functional status of some brain-injured patients. Given this progress and our increasing understanding of the neurobiology of the injured brain, functional imaging may play an important role in assessments of patients' potential for functional recovery.

## Acknowledgements

## References

Adams JH, Graham DI, Jennett B. The neuropathology of the vegetative state after an acute brain insult. Brain 2000; 123: 1327–38.

Alexander GE, DeLong MR, Strick PL. Parallel organization of functionally segregated circuits linking basal ganglia and cortex. [Review]. Annu Rev Neurosci 1986; 9: 357–81.

Alexander GE, Crutcher MD, De Long MR. Basal ganglia–thalamocortical circuits: parallel substrates for motor, oculomotor, 'prefrontal' and 'limbic' functions. [Review]. Prog Brain Res 1990; 85: 119–46.

Barrett AM, Crucian GP, Raymer AM, Heilman KM. Spared comprehension of emotional prosody in a patient with global aphasia. Neuropsychiatry Neuropsychol Behav Neurol 1999; 12: 117–20.

Baumgartner C, Deecke L, Stroink G, Williamson SJ. Bio-

magnetism: fundamental research and clinical applications. Amsterdam: Elsevier; 1995.

Baynes K, Eliassen J, Lutsep HL, Gazzaniga MS. Modular organization of cognitive systems masked by interhemispheric integration. Science 1998; 280: 902–5.

Benabid AL, Pollak P, Seigneuret E, Hoffmann D, Gay E, Perret J. Chronic VIM thalamic stimulation in Parkinson's disease, essential tremor and extra-pyramidal dyskinesias. Acta Neurochir Suppl (Wien) 1993; 58: 39–44.

Beresford HR. The persistent vegetative state: a view across the legal divide. [Review]. Ann NY Acad Sci 1997; 835: 386–94.

Bhatia KP; Marsden CD. The behavioural and motor consequences of focal lesions of the basal ganglia in man. Brain 1994; 117: 859–76.

Blacklock JB, Oldfield EH, Di Chiro G, Tran D, Theodore W, Wright DC, et al. Effect of barbituate coma on glucose utilization in normal brain versus gliomas. Positron emission tomography studies. J Neurosurg 1987; 67: 71–5.

Cairns H, Oldfield RC, Pennybacker JB, Whitteridge D. Akinetic mutism with an epidermoid cyst of the 3rd ventricle. Brain 1941; 64: 273–90.

Cannon, WB Bodily changes in pain, hunger, fear and rage, 2nd edn. New York: Harper & Row; 1929.

Castaigne P, Lhermitte F, Buge A, Escourolle P, Hauw JJ, Lyon-Caen O. Paramedian thalamic and midbrain infarcts: clinical and neuropathological study. Ann Neurol 1981; 10: 127–48.

Collignon A, Maes F, Delaere D. Automated multimodality image registration using information theory. In: Viergever MA, editor. Computational imaging and vision. Proceedings of the 13th International Conference, IPMI Vol. 3. Dordrecht: Kluwer Academic; 1995. p. 263–74.

Contreras D, Destexhe A, Sejnowski TJ, Steriade M. Control of spatiotemporal coherence of a thalamic oscillation by cortico-thalamic feedback. Science 1996; 274: 771–4.

de Jong BM, Willemsen AT, Paans AM. Regional cerebral blood flow changes related to affective speech presentation in persistent vegetative state. Clin Neurol Neurosurg 1997; 99: 213–6.

DeGrado TR, Turkington TG, Williams JJ, Stearns CW, Hoffman JM, Coleman RE. Performance characteristics of a whole-body PET scanner. J Nucl Med 1994; 35: 1398–406.

Desmedt JE, Tomberg C. Transient phase-locking of 40-Hz electrical oscillations in prefrontal and parietal human cortex reflects the process of conscious somatic perception. Neurosci Lett 1994; 168: 126–9.

DeVolder AG, Goffinet AM, Bol A, Michel C, de Barsy T, Laterre C. Brain glucose metabolism in postanoxic syndrome. Arch Neurol 1990; 47: 197–204.

Dhawan V, Kazumata K, Robeson W, Belakhlef A, Margouleff C, Chaly T, et al. Quantitative brain PET: comparison of 2D and 3D acquisitions on the GE Advance scanner. Clin Positron Imaging 1998; 1: 135–44.

Facon M, Steriade M, Wertheim N. Hypersomie prolonge engendere par des lesions bilatereles du systeme activateur

medial. Le syndrome thrombotique de la bifurcation du tronc basilaire. Rev Neurol (Paris) 1958; 98: 117–33.

Fins JJ. A proposed ethical framework for interventional cognitive neuroscience: a consideration of deep brain stimulation in impaired consciousness. [Review]. Neurol Res 2000; 22: 273–8.

Firsching R, Luther J, Eidelberg E, Brown WE, Story JL, Boop FA. 40 Hz–middle latency auditory evoked response in comatose patients. Electroencephalogr Clin Neurophysiol 1987; 67: 213–6.

Fisher CM. Honored guest presentation: abulia minor vs. agitated behavior. Clin Neurosurg 1983; 31: 9–31.

Giacino, JT, Ashwal, S, Childs, N, Cranford, R, Jennett, B, Katz, DI, et al. The minimally conscious state: definition and diagnostic criteria. Neurology. In press 2002.

Groenewegen HJ, Berendse HW. The specificity of the 'nonspecific' midline and intralaminar thalamic nuclei. Trends Neurosci 1994; 17: 52–7.

Hari R, Reinikainen K, Kaukoranta E, Hamalainen M, Ilmoniemi R, Penttinen A, et al. Somatosensory evoked cerebral magnetic fields from SI and SII in man. Electroencephalogr Clin Neurophysiol 1984; 57: 254–63.

Inbody S, Jankovic J. Hyperkinetic mutism: bilateral ballism and basal ganglia calcification. Neurology 1986; 36: 825–7.

Ingvar DH, Sourander P. Destruction of the reticular core of the brain stem. Arch Neurol 1970; 23: 1–8.

Jeanmonod D, Magnin M, Morel A. Low-threshold calcium spike bursts in the human thalamus. Common physiopathology for sensory, motor and limbic positive symptoms. Brain 1996; 119: 363–75.

Jennett B, Plum F. Persistent vegetative state after brain damage. A syndrome in search of a name. Lancet 1972; 1: 734–7.

Jennett B, Adams HJ, Murray LS, Graham DI. Neuropathology in vegetative and severely disabled patients after head injury. Neurology 2001; 56: 486–90.

Joliot M, Ribary U, Llinás R. Human oscillatory brain activity near 40 Hz coexists with cognitive temporal binding. Proc Natl Acad Sci USA 1994; 91: 11748–51.

Kampfl A, Franz G, Aichner F, Pfausler B, Haring HP, Ulmer H, Felber S, et al. The persistent vegetative state after closed head injury: clinical and magnetic resonance imaging findings in 42 patients. J Neurosurg 1998; 88: 809–16.

Kinney HC, Korein J, Panigrahy A, Dikkes P, Goode R. Neuropathological findings in the brain of Karen Ann Quinlan. N Engl J Med 1994; 330: 1469–75.

Kinomura S, Larssen J, Gulyas B, Roland PE. Activation by attention of the human reticular formation and thalamic intralaminar nuclei. Science 1996; 271: 512–5.

Laureys S, Goldman S, Phillips C, Van Bogaert P, Aerts J, Luxen A, et al. Impaired effective cortical connectivity in vegetative state: preliminary investigation using PET. Neuroimage 1999; 9: 377–82.

Levy DE, Sidtis JJ, Rottenberg DA, Jarden JO, Strother SC, Dhawan V, et al. Differences in cerebral blood flow and glucose utilization in vegetative versus locked-in patients. Ann Neurol 1987; 22: 673–82.

Liegeois-Chauvel C, Peretz I, Babai M, Laguitton V, Chauvel P. Contribution of different cortical areas in the temporal lobes to music processing. Brain 1998; 121: 1853–67.

Llinás RR. The intrinsic electrophysiological properties of mammalian neurons: insights into central nervous system function. [Review]. Science 1988; 242: 1654–64.

Llinás R, Ribary U. Coherent 40-Hz oscillation characterizes dream state in humans. Proc Natl Acad Sci USA 1993; 90: 2078–81.

Llinás RR, Ribary U. Temporal conjunction in thalamocortical transactions. [Review]. Adv Neurol 1998, 77: 95–103.

Llinás RR, Grace AA, Yarom Y. In vitro neurons in mammalian cortical layer 4 exhibit intrinsic oscillatory activity in the 10- to 50-Hz frequency range. Proc Natl Acad Sci USA 1991; 88: 897–901.

Llinás R, Ribary U, Joliot M, Wang XJ. Content and context in temporal thalamocortical binding. In: Buzsaki G, Llinás R, Singer W, Berthoz A, Christen Y, editors. Temporal coding in the brain. Berlin: Springer-Verlag; 1994. p. 251–72.

Llinás R, Ribary U, Contreras D, Pedroarena C. The neuronal basis for consciousness. [Review]. Philos Trans R Soc Lond B Biol Sci 1998a; 353: 1841–9.

Llinás R, Ribary U, Tallal P. Dyschronic language-based learning disability. In: Von Euler C, Lundberg, I, Llinás R, editors. Basic mechanisms in cognition and language. Amsterdam: Elsevier; 1998b. p. 101–8.

Llinás RR, Ribary U, Jeanmonod D, Kronberg E, Mitra PP. Thalamo-cortical dysrhythmia: a neurological and neuropsychiatric syndrome characterized by magnetoencephalography. Proc Natl Acad Sci USA 1999; 96: 15222–7.

Madler C, Keller I, Schwender D, Poeppel E. Sensory information processing during general anaesthesia: effect of isoflurane on auditory evoked neuronal oscillations. Br J Anaesth 1991; 66: 81–7.

Makela JP, Hari R. Evidence for cortical origin of the 40 Hz auditory evoked response in man. Electroencephalogr Clin Neurophysiol 1987; 66: 539–46.

Maquet P, Dive D, Salmon E, Sadzot B, Franco G, Poirrier R, et al. Cerebral glucose utilization during sleep–wake cycle in man determined by positron emission tomography and [18F]2-fluoro-2-deoxy-D-glucose method. Brain Res 1990; 513: 136–43.

Marrocco RT, Witte EA, Davidson, MC. Arousal systems. [Review]. Curr Opin Neurobiol 1994; 4: 166–70.

McCormick DA, Neurotransmitter actions in the thalamus and cerebral cortex. J Clin Neurophysiol 1992; 9: 212–23.

Menon DK, Owen AM, Williams EJ, Minhas PS, Allen CM, Boniface SJ, et al. Cortical processing in persistent vegetative state. Lancet 1998; 352: 200.

Mogilner A, Grossman JA, Ribary U, Joliot M, Volkmann J, Rapaport D, et al. Somatosensory cortical plasticity in adult humans revealed by magnetoencephalography. Proc Natl Acad Sci USA 1993; 90: 3593–7.

Mori E, Yamadori, A. Rejection behaviour: a human homologue of

the abnormal behaviour of Denny-Brown and Chambers' monkey with bilateral parietal ablation. J Neurol Neurosurg Psychiatry 1989; 52: 1260–6.

Moruzzi G, Magoun HW. Brainstem reticular formation and activation of the EEG. Electroencephalogr Clin Neurophysiol 1949; 1: 455–473.

Multi-Society Task Force on PVS. Medical aspects of the persistent vegetative state. Part 1. N Engl J Med 1994; 330: 1499–508.

Nakamura A, Yamada T, Goto A, Kato T, Ito K, Abe Y, et al. Somatosensory homunculus as drawn by MEG. Neuroimage 1998; 7: 377–86.

Nemeth G, Hegedus K, Molnar L Akinetic mutism associated with bicingular lesions: clinicopathological and functional anatomical correlates. Eur Arch Psychiatry Neurol Sci 1988; 237: 218–22.

NIH consensus development panel on rehabilitation of persons with traumatic brain injury. JAMA 1999; 282: 974–83.

Okada YC, Tanenbaum R, Williamson SJ, Kaufman L. Somatotopic organization of the human somatosensory cortex revealed by neuromagnetic measurements. Exp Brain Res 1984; 56: 197–205.

Owen AM, Menon DK, Williams EJ, Minhas PS, Johnsrude IS, Scott SK, et al. Detecting residual cognitive function in persistent vegetative state (PVS) using functional neuroimaging [abstract]. Soc Neurosci Abstr 1999; 25: 1091.

Panksepp J. Affective neuroscience. New York: Oxford University Press; 1998.

Pantev C, Hoke M, Lehnertz K, Lutkenhoner B, Anogianakis G, Wittkowski W. Tonotopic organization of the human auditory cortex revealed by transient auditory evoked magnetic fields. Electroencephalogr Clin Neurophysiol 1988; 69: 160–70.

Pantev C, Hoke M, Lütkenhöner B, Lehnertz K. Tonotopic organization of the auditory cortex: pitch versus frequency representation. Science 1989; 246: 486–8.

Pantev C, Makeig S, Hoke M, Galambos R, Hampson S, Gallen C. Human auditory evoked gamma-band magnetic fields. Proc Natl Acad Sci USA 1991; 88: 8996–9000.

Parent A, Hazrati LN. Functional anatomy of the basal ganglia. I. The cortico-basal ganglia-thalamo-cortical loop. [Review]. Brain Res Brain Res Rev 1995; 20: 91–127.

Pfurtscheller G, Neuper C. Event-related synchronization of mu rhythm in the EEG over the cortical hand area in man. Neurosci Lett 1994; 174: 93–6.

Pfurtscheller G, Schwarz G, Pfurtscheller B, List W. Computer assisted analysis of EEG, evoked potentials, EEG reactivity and heart rate variability in comatose patients. [German]. EEG EMG Z Elektroenzephalogr Elektromyogr Verwandte Geb 1983; 14: 66–73.

Phelps ME, Huang SC, Hoffman EJ, Selin C, Sokoloff L, Kuhl DE. Tomographic measurement of local cerebral glucose metabolic rate in humans with (F-18)2-fluoro-2-deoxy-D-glucose: validation of method. Ann Neurol 1979; 6: 371–88.

Plum, F. Coma and related global disturbances of the human conscious state. In: Peters, A, Jones, EG, editors. Cerebral cortex, Vol. 9. New York: Plenum Press. 1991. p. 359–425.

Plum F, Posner J. The diagnosis of stupor and coma, 3rd edn. Philadelphia: F.A. Davis; 1980.

Plum F, Schiff N, Ribary U, Llinas R. Coordinated expression in chronically unconscious persons. Philos Trans R Soc Lond B Biol Sci 1998; 353: 1929–33.

Purpura KP, Schiff, ND. The thalamic intralaminar nuclei: role in visual awareness. Neuroscientist 1997; 3: 8–14.

Regan D. Human brain electrophysiology: evoked potentials and evoked magnetic fields in science and medicine. New York: Elsevier; 1989.

Reite M, Zimmerman JT, Edrich J, Zimmerman JE. Auditory evoked magnetic fields: response amplitude vs. stimulus intensity. Electroencephalogr Clin Neurophysiol 1982; 54: 147–52.

Relkin NR, Petito CK, Plum F. Coma and the vegetative state associated with thalamic injury after cardiac arrest [abstract]. Ann Neurol 1990; 20: 21.

Rezai AR, Hund M, Kronberg E, Zonenshayn M, Cappell J, Ribary U, et al. The interactive use of magnetoencephalography in stereotactic image-guided neurosurgery. Neurosurgery 1996; 39: 92–102.

Ribary U, Llinás R, Kluger A, Suk J, Ferris SH. Neuropathological dynamics of magnetic, auditory, steady-state responses in Alzheimer's disease. In: Williamson SJ, Hoke M, Stroink G, Kotani M, editors. Advances in biomagnetism. New York: Plenum Press; 1989. p. 311–4.

Ribary U, Ioannides AA, Singh KD, Hasson R, Bolton JP, Lado F, et al. Magnetic field tomography of coherent thalamocortical 40-Hz oscillations in humans. Proc Natl Acad Sci USA 1991; 88: 11037–41.

Ribary U, Cappell J, Mogilner A, Hund-Georgiadis M, Kronberg E, Llinás R. Functional imaging of plastic changes in the human brain. [Review]. Adv Neurol 1999; 81: 49–56.

Romani GL, Williamson SJ, Kaufman L. Tonotopic organization of the human auditory cortex. Science 1982; 216: 1339–40.

Ross ED. The aprosodias. In: Feinberg TE, Farah MJ, editors. Behavioral neurology and neuropsychology. New York: McGraw-Hill; 1997. p. 699–710.

Rudolf J, Ghaemi M, Ghaemi M, Haupt WF, Szelies B, Heiss WD. Cerebral glucose metabolism in acute and persistent vegetative state. J Neurosurg Anesthesiol 1999; 11: 17–24.

Sarvas J. Basic mathematical and electromagnetic concepts of the biomagnetic inverse problem. Phys Med Biol 1997; 32: 11–22.

Sauvé K, Wang G, Rolli M, Jagow R, Kronberg E, Ribary U, et al. Human gamma-band brain activity covaries with cognitive temporal binding of somatosensory stimuli in sighted and blind subjects [abstract]. Soc Neurosci Abstr 1998; 24: 1128.

Schiff ND, Plum F. Target article: the neurology of impaired consciousness: global disorders and implied models. Association for the Scientific Study of Consciousness. Available from: http://athena.english.vt.edu/cgi-bin/netforum/nic/a/1

Schiff ND, Plum F. The role of arousal and 'gating' systems in the neurology of impaired consciousness. [Review]. J Clin Neurophysiol 2000; 17: 438–52

Schiff ND, Ribary U, Plum F, Llinás R. Words without mind. J Cogn Neurosci 1999; 11: 650–6.

Schiff ND, Rezai A, Plum F. A neuromodulation strategy for rational therapy of complex brain injury states. [Review]. Neurol Res 2000; 22: 267–72.

Segarra JM. Cerebral vascular disease and behavior. I. The syndrome of the mesencephalic artery (basilar artery bifurcation). Arch Neurol 1970; 22: 408–18.

Sokoloff L, Reivich M, Kennedy C, Des Rosiers MH, Patlak CS, Pettigrew KD, et al. The (14C) deoxyglucose method for the measurement of local cerebral glucose utilization: theory, procedure, and normal values in the conscious and anesthetized albino rat. J Neurochem 1977; 28: 897–916.

Spydell JD, Pattee G, Goldie WD. The 40 Hertz auditory event-related potential: normal values and effects of lesions. Electroencephalogr Clin Neurophysiol 1985; 62: 193–202.

Steriade M. Thalamic substrates of disturbances in states of vigilance and consciousness in humans. In: Steriade M, Jones EG, McCormick DA, editors. Thalamus, Vol. II. Amsterdam: Elsevier; 1997. p. 721–42.

Steriade M. Corticothalamic networks, oscillations and plasticity. Adv Neurol 1998; 77: 105–34.

Steriade M. Corticothalamic resonance, states of vigilance and mentation. [Review]. Neuroscience 2000; 101: 243–76.

Steriade M, Glenn LL. Neocortical and caudate projections of intralaminar thalamic neurons and their synaptic excitation from midbrain reticular core. J Neurophysiol 1982; 48: 352–71

Steriade, M, Llinás, RR. The functional states of the thalamus and the associated neuronal interplay. [Review]. Physiol Rev 1988; 68: 649–742.

Steriade M, Contreras D, Amzica F, Timofeev I. Synchronization of fast (30–40 Hz) spontaneous oscillations in intrathalamic and thalamocortical networks. J Neurosci 1996; 16: 2788–808.

Suk J, Ribary U, Cappell J, Yamamoto T, Llinás R. Anatomical localization revealed by MEG recordings of the human somatosensory system. Electroencephalogr Clin Neurophysiol 1991; 78: 185–96.

Sutherling WW, Crandall PH, Darcey TM, Becker DP, Levesque MF, Barth DS. The magnetic and electric fields agree with intracranial localizations of somatosensory cortex. Neurology 1988; 38: 1705–14.

Tommasino C, Grana C, Lucignani G, Torri G, Fazio, F. Regional cerebral metabolism of glucose in comatose and vegetative state patients. J Neurosurg Anesthesiol 1995; 7: 109–16.

Tononi G, Edelmann GM. Consciousness and complexity. [Review]. Science 1998; 282: 1846–51.

Weinberg H, Cheyne D, Brickett P, Harrop R, Gordon R. An interaction of cortical sources associated with simultaneous auditory and somesthetic stimulation. In: Pfurtscheller G, Lopes da Silva FH, editors. Functional brain imaging. Toronto: Hans Huber; 1988. p. 83–8.

Williamson SJ, Kaufman L. Evolution of neuromagnetic topographic mapping. [Review]. Brain Topogr 1990; 3: 113–27.

Wood CC, Spencer DD, Allison T, McCarthy G, Williamson PD, Goff WR. Localization of human sensorimotor cortex during surgery by cortical surface recording of somatosensory evoked potentials. J Neurosurg 1988; 68: 99–111.

Winslade WJ. Contronting traumatic brain injury. New Haven: Yale University Press 1998.

Yamamoto T, Williamson SJ, Kaufman L, Nicholson C, Llinás R. Magnetic localization of neuronal activity in the human brain. Proc Natl Acad Sci USA 1988; 85: 8732–6.